

*Studies in Radar*  
*Cross-Sections - VIII*

*Theoretical Cross-Sections as a Function  
of Separation Angle Between Transmitter  
and Receiver at Small Wavelengths*

*by K. M. Siegel, H. A. Alperin, R. R. Bonkowski,  
J. W. Crispin, A. L. Maffett, C. E. Schensted,  
and I. V. Schensted*

*Project MX-794*

*USAF Contract W33-038-ac-14222*

*Second Printing, June, 1954*

*Willow Run Research Center  
Engineering Research Institute  
University of Michigan  
UMM-115    October, 1953*

## STUDIES IN RADAR CROSS-SECTIONS

- I Scattering by a Prolate Spheroid by F. V. Schultz (March 1950).
- II The Zeros of the Associated Legendre Functions  $P_n^m(\mu')$  of Non-Integral Degree by K. M. Siegel, D. M. Brown, H. E. Hunter, H. A. Alperin, and C. W. Quillen (April 1951).
- III Scattering by a Cone by K. M. Siegel and H. A. Alperin (January 1952).
- IV Comparison Between Theory and Experiment of the Cross-Section of a Cone by K. M. Siegel, H. A. Alperin, J. W. Crispin, H. E. Hunter, R. E. Kleinman, W. C. Orthwein, and C. E. Schensted (February 1953).
- V A classified paper on bistatic radars by K. M. Siegel (August 1952).
- VI Cross-Sections of Corner Reflectors and Other Multiple Scatterers by R. R. Bonkowski, C. R. Lubitz, and C. E. Schensted (October 1953).
- VII A classified summary report by K. M. Siegel, J. W. Crispin, and R. E. Kleinman (November 1952).
- VIII Theoretical Cross-Sections as a Function of Separation Angle Between Transmitter and Receiver at Small Wavelengths by K. M. Siegel, H. A. Alperin, R. R. Bonkowski, J. W. Crispin, A. L. Maffett, C. E. Schensted, and I. V. Schensted (October 1953).
- IX Electromagnetic Scattering by an Oblate Spheroid by L. M. Rauch (October 1953).
- X The Radar Cross-Section of a Sphere by H. Weil (to be published).
- XI The Numerical Determination of the Radar Cross-Section of a Prolate Spheroid by K. M. Siegel, B. H. Gere, I. Marx, and F. B. Sleator (December 1953).
- XII A classified summary report by K. M. Siegel, M. E. Anderson, R. R. Bonkowski, and W. C. Orthwein (December 1953).

## TABLE OF CONTENTS

Section	Title	Page
	List of Figures	iii
	List of Tables	iii
	Nomenclature	iv
	Preface	viii
I	Introduction and Summary	1
II	Approximation Methods	3
	2.1: A Discussion of the Application of Physical-Optics Approximations	3
	2.2: The Choice of Method	6
III	Physical Optics and the Determination of Bistatic Cross-Sections	9
	3.1: Basic Assumptions of Physical Optics	9
	3.2: Application of the Physical-Optics Method to Bistatic Cross-Sections	10
	3.3: Reciprocity Relationships and the Current-Distribution Method	15
IV	The Bistatic Cross-Section of Finite Surfaces of Revolution With the Transmitter Located on the Axis of Symmetry of the Body	20
	4.1: The Prolate Spheroid	21
	4.2: The Sphere	22
	4.3: The Ogive	25
	4.4: The Finite Cone	32
V	The Bistatic Cross-Section of Semi-Infinite Surfaces of Revolution With the Transmitter Located on the Axis of Symmetry	36
	5.1: The Paraboloid	36
	5.2: The Semi-Infinite Cone	37
VI	Bistatic Cross-Sections For Arbitrary Transmitter and Receiver Directions	46
	6.1: The Elliptic Cylinder	46

## TABLE OF CONTENTS (Continued)

Section	Title	Page
6.2:	The Prolate and Oblate Spheroids for Particular Choices of Transmitter and Receiver Directions	51
6.3:	Determination of $\sigma$ by Numerical Integration Techniques	56
VII	Conclusion	61
Appendix 1 -	Proof of the Double Stationary-Phase Theorem	63
Appendix 2 -	Determination of $\sigma_{\hat{a}=\hat{y}}^{\hat{a}}(\beta)$ by the D.S.P. Theorem for the Prolate Spheroid, the Sphere, and the Ogive	68
Appendix 3 -	The Hansen and Schiff Treatment of Back Scattering from a Spindle	72
Appendix 4 -	The Luneberg-Kline Method	75
Appendix 5 -	Cross-Section Formulas for Other Surfaces	79
References		81

UMM-115

## LIST OF FIGURES

Figure No.	Title of Figure	Page
Figure 1	The Angle $\beta$	1
Figure 2	Back-Scattering From a Perfectly Conducting Sphere	4
Figure 3	Basic Geometry for Surfaces of Revolution	13
Figure 4	Projections of Shadow Curves and Regions of Integration	17
Figure 5	Cross-Section of a Prolate Spheroid as a Function of $\beta$	23
Figure 6	Cross-Section of a Sphere as a Function of $\beta$	24
Figure 7	Geometry for the Ogive	25
Figure 8	Cross-Section of an Ogive of Half-Angle $\alpha$ and Length L as a Function of $\beta$	30
Figure 9	Cross-Section of an Ogive of Half-Angle $15^\circ$ and Maximum Diameter Equal to $100 \lambda/\pi$	31
Figure 10	Cross-Section of a Finite Cone of Half-Angle $\gamma$	35
Figure 11	The Bistatic Cross-Section of a Paraboloid	38
Figure 12	Geometry for Semi-Infinite Cone	39
Figure 13	Bistatic Cross-Section of a Semi-Infinite Cone of Half-Angle $15^\circ$	45
Figure 14	Geometry for the Elliptic Cylinder	46
Figure 15	Bistatic Cross-Section of an Elliptic Cylinder	52
Figure 16	Geometry for Prolate Spheroid	55
Figure 17	Bistatic Cross-Section of a Prolate Spheroid	57

## LIST OF TABLES

Table 1	Approximate Monostatic and Bistatic Cross-Section Formulas	62
Table 2	Other Approximate Monostatic Cross-Section Formulas	79
Table 3	Other Approximate Bistatic Cross-Section Formulas	80

## NOMENCLATURE\*

$A$	= semi-major axis of prolate spheroid. (A is also used as a condensation symbol.)
$A_r, A_t$	= projections of regions of integration in the direction of the receiver and transmitter respectively.
$A(\rho)$	= area of surface up to phase plane whose position is determined by $\rho$
$B$	= semi-minor axis of prolate spheroid. (B is also used as a condensation symbol.)
$\vec{F}$	= a vector used in defining $\sigma(\beta)$ .
$\vec{E}_1, \vec{E}_2$	= electric field vectors (used in discussion of reciprocity).
$H_0$	= amplitude of the incident magnetic field vector.
$\vec{H}_{sc}$	= the scattered magnetic field vector.
$\vec{H}_t$	= the tangential component of the magnetic field on the scattering surface.
$\overset{\wedge}{I}$	= the unit dyadic.
$I_x, I_y, I_z$	= the x, y, and z components of a vector.
$\vec{J}_1 e^{i\omega t}, \vec{J}_2 e^{i\omega t}$	= current distributions (used in discussion of reciprocity).
$J_\nu(u)$	= the cylindrical Bessel function of degree $\nu$ and argument $u$ .
$L$	= the maximum dimension of the scattering body. (L is also used to denote the length of the ogive and the length of the elliptic cylinder).
$R_0$	= radius of a sphere.

\*Does not include symbols employed in the appendices or in the D.S.P. Theorem.

## NOMENCLATURE (Continued)

$R_1, R_2$	= principal radii of curvature of a surface at a point.
$R$	= the distance separating the receiver and the integration point on the surface.
$R'$	= the distance separating the receiver and the origin of the coordinate system.
D.S.P.	= the double stationary-phase theorem.
$\hat{a}$	= a unit vector in the direction of the incident magnetic field. ( $\hat{a}$ has the components $a_x$ , $a_y$ , and $a_z$ .)
$a$	= semi-major axis of elliptic cylinder. ( $a$ is also used as a condensation symbol.)
$b$	= semi-minor axis of elliptic cylinder. ( $b$ is also used as a condensation symbol.)
$\hat{c}$	= direction of semi-infinite cone axis.
$c$	= a constant. ( $c$ is also used as a condensation symbol.)
$d$	= the maximum diameter of the ogive.
$\hat{d}$	= direction of polarization at the receiver.
$\vec{i}_t$	= $\hat{a} - (\hat{a} \cdot \hat{n})\hat{n}$ .
$i$	= $\sqrt{-1}$ .
$\hat{i}_x, \hat{i}_y, \hat{i}_z$	= unit vectors along the x, y, and z axes respectively.
$k$	= $2\pi/\lambda$ .
$\hat{k}$	= unit vector directed from the transmitter, assumed to be infinitely far away, to the origin of the coordinate system.
$\hat{k}_1$	= $-\hat{k}$ .
$l$	= the characteristic dimension of the body.
$\hat{n}$	= unit vector normal to the surface, with components $n_x$ , $n_y$ , and $n_z$ .

## NOMENCLATURE (Continued)

$\hat{n}_o$	= unit vector directed from receiver to origin, with components $n_{ox}$ , $n_{oy}$ , and $n_{oz}$ .
$\hat{n}'_o$	= $-\hat{n}_o$ .
$p$	= radius of circle whose arc is used in obtaining equation of the ogive; the equation of the circle in the $w$ - $z$ plane is $(w + h)^2 + z^2 = p^2$ . ( $p$ is also used to denote the distance from the focus to the vertex in the discussion of the paraboloid.)
$\vec{r}$	= radius vector from the origin to a point on the scattering surface.
$\vec{r}_1, \vec{r}_2$	= vectors which define the location of transmitter and receiver in the discussion of reciprocity.
$r_o$	= slant length of finite cone.
$\alpha$	= 1/2 nose-angle of the ogive.
$\alpha_o$	= $\text{Cos}^{-1} \left( - \frac{\hat{n}_o \cdot \vec{r}}{ \vec{r} } \right)$ .
$\beta$	= the angle separating the transmitter and receiver.
$\beta_1$	= angle used in discussion of spheroids (see Fig. 15).
$\gamma$	= 1/2 nose-angle of cone.
$\delta$	= variable used in obtaining the Abelian limit.
$\lambda$	= the wavelength.
$\left. \begin{array}{l} \theta_r, \theta_t \\ \phi_r, \phi_t \end{array} \right\}$	= angles used in defining the location of the transmitter and receiver in the discussion of the elliptic cylinder.
$\phi$	= angle between plane of polarization of the incident field and the plane containing the axis of the cone and the receiver.
$\sigma_e(\beta)$	= the effective cross-section.
$\sigma(\beta)$	= the radar cross-section for the case in which the transmitter and receiver are separated by the angle $\beta$ .



## NOMENCLATURE (Continued)

- $\sigma(o)$  = the back-scattering cross-section.
- $\sigma_{\hat{a}=\hat{1}_y}^{\hat{a}}(\beta)$  = the bistatic cross-section for the case in which the transmitter is located on the axis of symmetry of the body and the polarization at the transmitter is in the direction  $\hat{1}_y$ .
- $\sigma_o$  = "true" cross-section for a pair of reciprocal cases.
- $\sigma_1, \sigma_2$  = two approximations to  $\sigma_o$  for reciprocal cases obtained using the current distribution method.
- $\sigma_1^*, \sigma_2^*$  = two approximations to  $\sigma_o$  for reciprocal cases using that portion of the surface "seen" by both receiver and transmitter as the region of integration.

## Miscellaneous

$D, G_1, G_2, G_3, \alpha', \theta', f(w),$  and  $g(\phi)$  = condensation symbols.

$\phi, \theta, w, r, \rho, \xi,$  and  $\eta$  = variables of integration.

## PREFACE

This paper is the eighth in a series of reports growing out of studies of radar cross-sections at the University of Michigan's Willow Run Research Center. The primary aims of this program are:

- (1) To show that radar cross-sections can be determined analytically.
- (2) To elaborate means for computing cross-sections of objects of military interest.
- (3) To demonstrate that these theoretical cross-sections are in agreement with experimentally determined values.

Intermediate objectives are:

- (1) To compute the exact theoretical cross-sections of various simple bodies by solution of the appropriate boundary-value problems arising from the electromagnetic vector wave equation.
- (2) To examine the various approximations possible in this problem, and determine the limits of their validity and utility.
- (3) To find means of combining the simple body solutions in order to determine the cross-sections of composite bodies.
- (4) To tabulate various formulas and functions necessary to enable such computations to be done quickly for arbitrary objects.
- (5) To collect, summarize, and evaluate existing experimental data.

Titles of the papers already published or presently in process of publication are listed on the back of the title page.

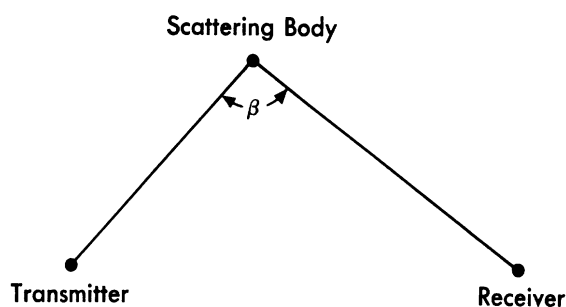
K. M. Siegel

## I

## INTRODUCTION AND SUMMARY

In this paper, bistatic radar cross-sections of simple configurations are obtained by applying an approximation method. In most of the cases considered the configuration is a surface of revolution, the transmitter is located on the axis of symmetry of the body, the polarization is specified, and the position of the receiver is allowed to vary in the plane of the axis of the body and the receiver.

The physical description of bistatic cross-sections differs from that of monostatic cross-sections in that the receiver and transmitter are permitted to be located at separate positions. To specify the bistatic radar cross-section of a body for a general location of transmitter and receiver more than one angle is required. However for most cases discussed in this paper, one angle, the angle  $\beta$  shown in Figure 1, suffices.

FIG. 1 THE ANGLE  $\beta$ 

The bistatic radar cross-section, therefore, is denoted by  $\sigma(\beta)$ . It is evident that the monostatic back-scattering radar cross-section is a special case ( $\beta = 0$ ) of the bistatic radar cross-section and can be denoted by  $\sigma(0)$ .

The approximation technique used is the current-distribution or physical-optics method. This method is applicable when the wavelength of the incident radiation is small with respect to the characteristic dimension of the body and is, in fact, a much better approximation technique than many have previously believed. Tests of the validity of this method and an explanation of why it may sometimes give better results in electromagnetic theory than in acoustics are discussed in Section 2.

The formulas of physical optics applicable to the bistatic radar cross-section problem, the stationary-phase technique for evaluating the integrals encountered, and the applicability of the reciprocity theorem of electromagnetic theory are discussed in Section 3. The physical-optics method is then applied in determining bistatic cross-sections for various finite and infinite surfaces of revolution for various receiver and transmitter locations (Sec. 4, 5, and 6). In the case of the paraboloid with the incident Poynting vector along the axis of symmetry it is shown that this method yields the exact bistatic result. The results obtained for these geometric shapes have been collected for easy reference in the conclusion (Sec. 7). This compilation is the first catalog of bistatic radar cross-section formulas. Monostatic formulas are included to increase the value of the table to the research worker.

## II

## APPROXIMATION METHODS

## 2.1: A Discussion of the Application of Physical-Optics Approximations

In using any approximation method it is desirable to know how the results obtained from it compare with the physically expected or experimental results. In determining the monostatic radar cross-section, when the wavelength is much less than the characteristic dimension of the body, the current-distribution method has provided many results which are in close agreement with experiment and with exact theoretical solutions. In the study of radar cross-sections, an approximation may be considered adequate if it is within a factor of ten of the correct answer.

In the case of the paraboloid (Sec. 5.1) the current-distribution method (incident Poynting vector on axis of symmetry) yields a bistatic result which is identical with the corresponding exact answer.

In the case of the sphere the bistatic result obtained by the current-distribution method is in close agreement with the exact answer for  $0 \leq \beta < 120^\circ$  and  $R_0/\lambda \gg 1$  where  $R_0$  is the radius of the sphere and  $\lambda$  is the wavelength (Ref. 1). As an example of the magnitudes of the differences encountered between physical-optics and exact-theory results, consider back-scattering from a perfectly conducting sphere. Both the exact and the physical-optics back-scattering cross-sections for the sphere and the envelopes of these curves are shown in Figure 2 (Ref. 1). It can be seen from this figure that the maximum error obtained in using the physical-optics approximation of  $\sigma$  is less than 40 per cent of  $\pi R_0^2$  and the average error is less than 25 per cent of  $\pi R_0^2$  providing  $R_0/\lambda > 1$ . The physical-optics result, therefore, approximates the exact solution of the sphere in the back-scattering case rather well for  $R_0/\lambda > 1$  and, as  $R_0/\lambda$  increases, the physical-optics result approaches the electromagnetic theory result. In this particular case it is apparent that the maximum error one would make in using the geometric-optics result over the range  $R_0/\lambda > 1$  would be even less than that obtained using physical-optics.

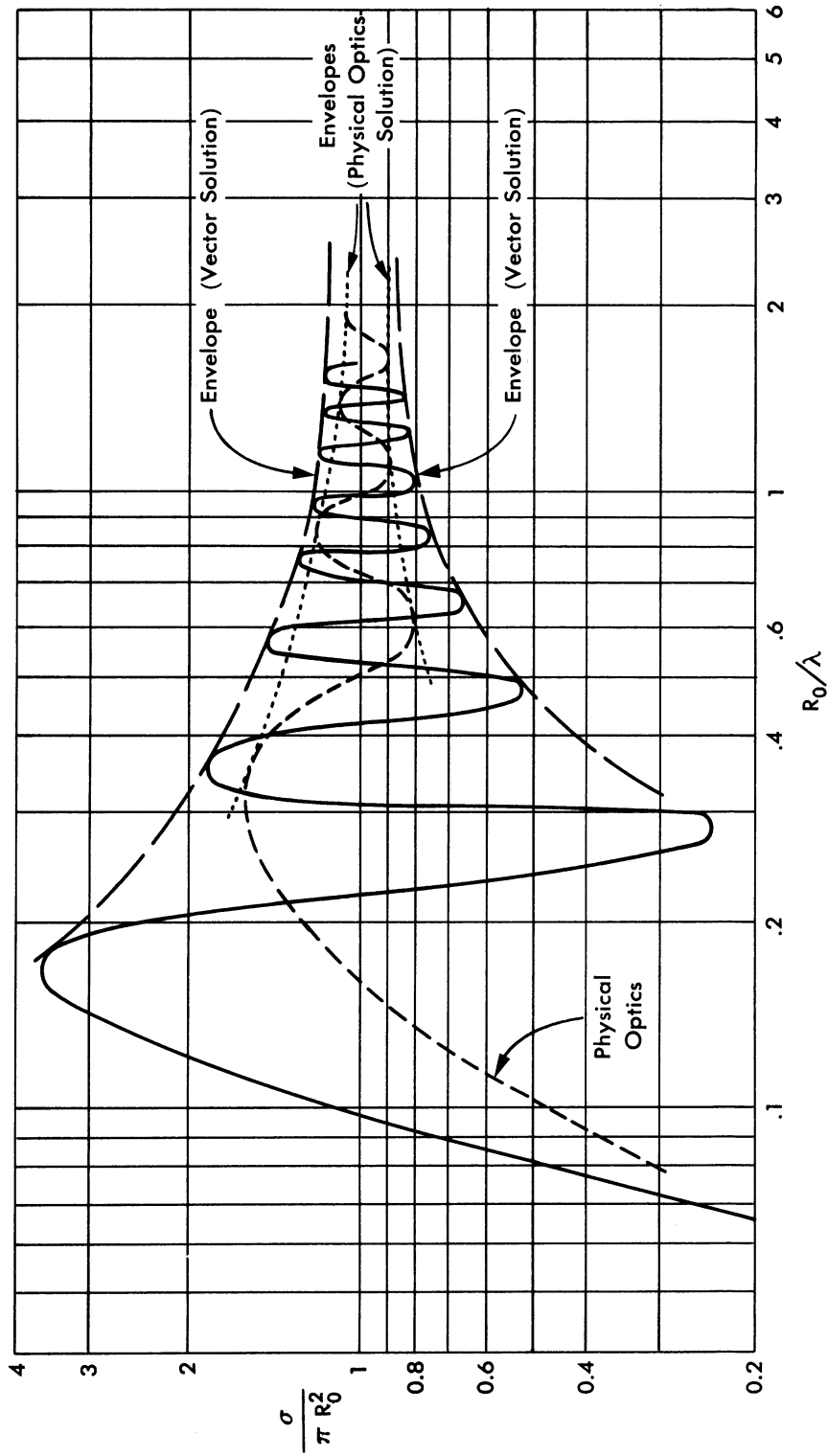


FIG. 2 BACK-SCATTERING FROM A PERFECTLY CONDUCTING SPHERE OF RADIUS  $R_0$

The current-distribution method (sometimes referred to as a Kirchhoff procedure) has been subjected to much criticism on both theoretical and experimental grounds (Refs. 2 and 3). For example, reasoning based on the assumptions of the current-distribution method listed in Section 3.1 would lead to the conclusion that this method should not be used when the surface has a point discontinuity. However, the method predicts the nose-on back-scattering cross-section of a semi-infinite cone to within experimental accuracies, if not exactly (Ref. 5).

In this paper, an Abelian limit process is used to determine the cross-section of a cone by a physical-optics approximation. When solving far zone problems for which the bodies are infinite in the direction of propagation, Abelian limit processes usually are convenient unless the configuration's tangent at infinity is parallel or perpendicular to the propagation vector. The limit process is commonly used, because it is not possible to get infinitely far from an infinite body. If the viscosity or conductivity of the medium is introduced into the problem (although these quantities may be negligible), then the problem becomes formally the same as the previous one with the objection to the limit process removed.

Some doubt has been thrown on the applicability of the physical-optics approximations to electromagnetic scattering problems in the past by the assertion that these approximations would always be in error by more than the corresponding physical-optics approximations to the acoustic problem. At least one apparent contradiction to this assertion has been developed in the present series of papers (Ref. 5), where it has been shown that physical optics predicts the exact electromagnetic cross-section for cones or small angle, whereas the same approximate methods predict a value four times as great as that predicted by the acoustic wave equation. Although the quantitative theoretical explanation of this factor of four cannot be elaborated at the present time, it is clear that such a disagreement should not be unexpected.

The acoustic wave equation which has been used is merely an approximation to the exact equation of the motion. This approximation is valid only when the wavelength is large (in comparison to the dimensions of the scatterer), because the influence of viscosity in acoustics is greatest at small wavelengths (Ref. 6). However, the physical-optics

approximation is valid only when the wavelength is small (in comparison to the dimensions of the scatterer). Hence the physical-optics approximation cannot be expected to reproduce accurately the real situation of acoustic scattering at any wavelength, whereas the same approximation can be expected to reproduce accurately the real situation in electromagnetic scattering whenever the wavelength is small.

Although in the above only an infinite body was under discussion, there is nothing in the argument which requires that the surface be infinite; the same type of conclusion would be reached for a finite body in a real fluid.

The cone result shows that it is possible to treat at least some pointed bodies by the current-distribution method. There is no proof available at the present time that pointed bodies in general can be treated by physical optics. Such a proof would require a stronger basis than the present existence and uniqueness proofs in electromagnetic theory, since the papers of Weyl and Müller (Ref. 7 and 8) and the Fredholm Theory are based on the assumption that the body is "sufficiently smooth".

In addition to the cone solution, a point (or rather 4 point singularities) has been treated by Kouyoumjian in his solution for the cross-section of a square flat plate (Ref. 4) by the Levine-Schwinger variational procedure (Ref. 9). The physical-optics result was in fairly good agreement with the variational result in the region where the wavelength was equal to or less than the side length of the scatterer. Kouyoumjian's experimental results agree more closely with the variational curve than with the physical-optics curve, but no great error would be made if the optics result were used.

In addition, the physical-optics determination of the nose-on back-scattering cross-section of an ogive (still another pointed body) is also in close agreement with experimental results (Ref. 5).

## 2.2: The Choice of Method

The introduction of an approximation method into a problem implies that it is felt that the determination of the exact solution is either



impossible or at least is much more difficult than the application of the approximation technique. This is certainly the case, for most configurations, in the radar cross-section problem. Yet the evidence presented in Section 2.1 indicates that, for small wavelengths, the current-distribution method yields results which are in close enough agreement with exact theory and/or experiment so as to be adequate for most practical purposes.\*

Thus the choice-of-method problem involved in this paper reduces to a question of how the integrals obtained in the current-distribution method are to be evaluated. For smooth bodies such as the sphere, the paraboloid, and the prolate spheroid, the stationary-phase method (Sections 3 and 4) is probably the best method to use except for fields in and near the shadow region. In Section 4 of this paper, the scattering cross-sections are determined by evaluating the physical-optics integrals both by the method of stationary phase and by use of analog computing equipment.\*\* The results obtained show that no clear case can be made for using the analog answer (physical-optics) rather than the stationary-phase (geometric-optics) evaluation for these bodies for a wide range of the angle  $\beta$ . There is however, some value in obtaining the physical-optics answer even though in the end result only the geometric-optics result will be used. The value lies in obtaining a "feel" for the wavelength dependence. In some cases it will even be possible to estimate the error from this crude dependence (See Fig. 2).

For a surface whose first and second derivatives are continuous, the essential contribution to the cross-section for short wavelengths can be obtained from the integral formulation of the current-distribution method if the integration is performed by the method of stationary phase. If the integration is performed exactly, a result dependent upon wavelength is usually obtained. Since the application of the method of stationary phase and the physical-optics integrals depend on the parameter

---

\*The procedure involved in the determination of exact electromagnetic theory cross-section is illustrated in the first, fourth, ninth, tenth, and eleventh papers in this series on "Studies in Radar Cross-Sections."

\*\*Analog equipment was chosen over other machine techniques after a thorough examination of all available methods.

$(k\ell)^{-1}$ , where  $k = 2\pi/\lambda$ ,  $\ell$  is the characteristic dimension of the body, and  $\lambda$  is the wavelength, it can be shown that the physical-optics result is a perturbation of the geometric-optics (or stationary-phase) result.

For a pointed body, the method of stationary-phase cannot be applied directly. The back-scattering cross-section predicted by geometric-optics is equal to  $\pi R_1 R_2$ , where  $R_1$  and  $R_2$  are the two radii of curvature. Hence, if a finite body has a point singularity, its cross-section by geometric optics would be zero. In this case, the physical-optics answer cannot be obtained from the geometric-optics answer by perturbation because there is no non-zero solution to perturb. A solution can, however, be obtained by integrating the surface integrals obtained exactly in one variable and by stationary phase in the other.

## III

PHYSICAL OPTICS AND THE DETERMINATION  
OF BISTATIC CROSS-SECTIONS

## 3.1: Basic Assumptions of Physical Optics

In order to apply the method of physical optics, it is necessary to make simplifying assumptions about the incident wave and the body. The exact nature of these assumptions depends to a large degree on the problem under consideration and, hence, the basic assumptions quoted in the literature differ from author to author. For example, consider the assumptions made by Spencer (Ref. 10) and by Milazzo (Ref. 11). The simplifying assumptions made by Spencer are:

- S1. "The incident wave is plane."
- S2. "The surface is perfectly conducting."
- S3. "The current distribution over the illuminated region of the body is obtained on the assumption that at every point the incident field is reflected as though an infinite plane wave were incident on the infinite tangent plane."
- S4. "The element of surface area is continuous with neighboring elements so that currents in a given element are independent of discontinuities in neighboring elements. This is a valid assumption for smooth surfaces with radii of curvature at least as large as a wavelength."

The assumptions made by Milazzo are:

- M1. "The scattering surface dimensions are large compared to the wavelength."
- M2. "The scattering surface is smooth, containing no abrupt corners, except possibly at extreme edges."

M3. "The scatterer is made of perfectly conducting material."

M4. "The incident wave is plane."

Assumptions S1 and M4 and S2 and M3 are identical, while assumptions S4 and M2 are identical with the exception of the condition "except possibly at the extreme edges" if it is assumed that both authors use the term "smooth" in the same way. However, assumptions S3 and M1 are not in general equivalent.

In this report, the assumptions made are stated as required. In most cases they are those made by Spencer.

### 3.2: Application of the Physical-Optics Method to Bistatic Cross-Sections

If the surface of the scattering body is assumed to be perfectly conducting (S2 or M3), the equation for the scattered magnetic field (Ref. 12, p. 466) can be written as

$$\vec{H}_{sc} = \frac{1}{4\pi} \int_s (\hat{n} \times \vec{H}_t) \times \nabla \left( \frac{e^{-ikR}}{R} \right) ds \quad (3.2-1)$$

where  $\vec{H}_{sc}$  = the scattered magnetic field vector,

$\hat{n}$  = the unit normal to the surface,

$\vec{H}_t$  = the tangential component of the magnetic field on the scattering surface,

R = the distance separating the receiver and the integration point,

k =  $2\pi/\lambda$  ( $\lambda$  = wavelength),

and s = the region of integration = the entire surface of the scatterer.

By assumption S3,  $\vec{H}_t$  can be approximated as twice the tangential component of the incident magnetic field on the "illuminated" side of the

body and zero on the "shadow" side of the body.\* Letting the incident magnetic field have a magnitude  $H_0$  and a direction  $\hat{a}$ , then according to this approximation,

$$\vec{H}_t = 2 \vec{i}_t H_0 e^{-ik(\hat{k} \cdot \vec{r})} \quad \text{on the "illuminated" side of the body,} \quad (3.2-2)$$

$$= 0 \quad \text{on the "shadow" side of the body,}$$

where  $\hat{k}$  = a unit vector directed from the transmitter, assumed to be infinitely far away, to the origin of the coordinate system,

$\vec{r}$  = the radius vector from the origin to any point on the surface of the scatterer, and

$$\vec{i}_t = \hat{a} - (\hat{a} \cdot \hat{n})\hat{n}.$$

If the receiver is at a very great distance from the body and if the body is finite, the following approximations are obtained:

$$\nabla \left( \frac{e^{-ikR}}{R} \right) \approx \frac{-ik}{R'} \left( e^{-ikR} \right) \hat{n}_0 \quad (3.2-3)$$

$$\text{and } R \approx R' - r \cos \alpha_0$$

where  $R'$  = the distance from the origin to the receiver,

$\hat{n}_0$  = the unit vector directed from the receiver to the origin, and

$$\cos \alpha_0 = -\frac{\hat{n} \cdot \vec{r}}{|\vec{r}|}.$$

If the incident magnetic field is of unit magnitude, then the substitution of (3.2-2) and (3.2-3) into (3.2-1) yields

$$\vec{H}_{sc} = \frac{\exp(-ikR')}{R'} \vec{F}(\beta) \quad (3.2-4)$$

\*The "shadow" curve is the locus of points on the body for which  $\hat{k} \cdot \hat{n} = 0$ . This curve separates the portion of the body "seen" by the transmitter, i.e., the "illuminated" side, from the "shadow" side.

where

$$\vec{F}(\beta) = \frac{ik}{2\pi} \left[ (\hat{n}_o \cdot \hat{a}) \vec{f} - (\hat{n}_o \cdot \vec{f}) \hat{a} \right]$$

and

$$\vec{f} = \int_{\hat{n}_e} -ik\vec{r} \cdot (\hat{n}_o + \hat{k}) ds = \hat{i}_x I_x + \hat{i}_y I_y + \hat{i}_z I_z .$$

illuminated  
region of  
the body

The radar cross-section is given by (Ref. 13)

$$\sigma(\beta) = 4\pi \left[ |F_x|^2 + |F_y|^2 + |F_z|^2 \right] . \tag{3.2-5}$$

The amount of energy received is proportional to the square of the magnitude of the scalar product of the vectors  $\vec{H}_{sc}$  and  $\hat{d}$ , where  $\hat{d}$  is the direction of the receiver polarization. It is convenient to define the effective cross-section as

$$\begin{aligned} \sigma_e(\beta) &= 4\pi \left| \vec{F} \cdot \hat{d} \right|^2 \\ &= \frac{4\pi}{\lambda^2} \left| (\hat{n}_o \cdot \hat{a}) (\vec{f} \cdot \hat{d}) - (\hat{n}_o \cdot \vec{f}) (\hat{a} \cdot \hat{d}) \right|^2 . \end{aligned} \tag{3.2-6}$$

If  $\hat{d}$  is given by a vector whose components are proportional to the complex conjugates of the corresponding components of  $\vec{F}$ , then  $\sigma_e(\beta)$  reduces to  $\sigma(\beta)$ .

If the body is a surface of revolution (the axis of symmetry taken to be the z-axis), there is no loss of generality if the receiver is restricted

to be in the  $yz$ -plane with  $y \leq 0$ . If in addition the transmitter is located on the  $z$ -axis ( $z > 0$ ), then the geometry shown in Figure 3 applies.

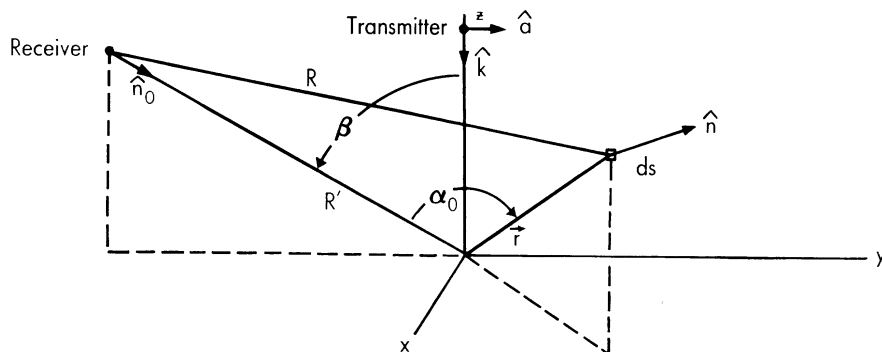


FIG. 3 BASIC GEOMETRY FOR SURFACES OF REVOLUTION

With the situation as pictured in Figure 3

$$\begin{aligned} \hat{n}_o &= \hat{i}_y \sin\beta - \hat{i}_z \cos\beta, \text{ and} \\ \hat{k} &= -\hat{i}_z. \end{aligned} \tag{3.2-7}$$

If the polarization of the incident wave is  $\hat{a} = \hat{i}_y$  and if the surface is symmetric with respect to the  $yz$ -plane, then

$$\sigma_{\hat{a}=\hat{i}_y}^{\hat{a}=\hat{i}_y}(\beta) = \frac{4\pi}{\lambda^2} |I_z|^2 \tag{3.2-8}$$

where  $I_z = \iint_{\text{illuminated region of body}} n_z \exp \left[ -ik\vec{r} \cdot (\hat{n}_o + \hat{k}) \right] ds.$

In many cases the integral  $I_z$  can be evaluated easily with the aid of the following double stationary-phase theorem (hereafter this theorem will be referred to as the D.S.P. theorem) which is proved in Appendix 1.

Let

$$I = \int_c^d \int_a^b f(x, y) e^{ikg(x, y)} dx dy.$$

If 1)  $f(x, y) = X(x) Y(y)$  is analytic in the region

$$R = \left\{ x, y \mid a \leq x \leq b, c \leq y \leq d \right\},$$

2)  $g(x, y)$  is analytic in  $R$ ,

3) there exists one and only one point  $(x_0, y_0)$ , in the interior of  $R$ , such that  $p_0 = q_0 = 0$  and  $r_0 t_0 - s_0^2 \neq 0$ , where  $p, q, r, s,$  and  $t$  are the usual partial derivatives of  $g$ ,\* and

4)  $X(\xi) / g_\xi(\xi, \eta)$  and  $Y(\eta) / g_\eta(\xi, \eta)$  are of bounded variation for  $(\xi, \eta)$  in  $R$  but not in

$$R' = \left\{ x, y \mid x_0 - \delta \leq x \leq x_0 + \delta, y_0 - \epsilon \leq y \leq y_0 + \epsilon \right\},$$

then

$$I = \pm \frac{2i \pi e^{ikg(x_0, y_0)} f(x_0, y_0)}{k [r_0 t_0 - s_0^2]^{1/2}} + O\left(\frac{1}{k^{3/2}}\right) \text{ as } k \rightarrow \infty$$

If  $I_z$  in (3.2-8) is evaluated by the method of stationary phase, the resulting value of cross-section is equal, in the limit as  $\lambda$  approaches zero, to the cross-section obtained by geometric optics. That is,

---

\*That is  $p = g_x, q = g_y, r = g_{xx}, s = g_{xy},$  and  $t = g_{yy}.$



evaluation of the physical-optics integral by the D.S.P. theorem leads to the geometric-optics answer.

### 3.3: Reciprocity Relationships and the Current-Distribution Method

It is sometimes possible, by known methods, to solve the bistatic problem if the transmitter is located on the axis of symmetry but not otherwise. Since it is often of more interest to have the receiver located in this position, a reciprocity theorem is presented which allows the cross-section to be determined for given positions of the transmitter and receiver if the problem has been solved with these positions interchanged.

It has been shown (Ref. 14) that for a field with time dependence  $e^{i\omega t}$  incident on a perfect conductor of finite dimensions

$$\oiint_{S_\infty - C} (\vec{E}_1 \cdot \vec{J}_2 - \vec{E}_2 \cdot \vec{J}_1) dV = 0 \quad (3.3-1)$$

where  $S_\infty$  is a sphere of infinite radius,

$C$  is the scattering surface,

$\vec{J}_1 e^{i\omega t}$  and  $\vec{J}_2 e^{i\omega t}$  define the current distributions in the two reciprocal cases ( $\vec{J}_1$  and  $\vec{J}_2$  are assumed to vanish except in the vicinity of  $\vec{r}_1$  and  $\vec{r}_2$ , the locations of the transmitter and receiver),

and  $\vec{E}_1$  and  $\vec{E}_2$  are the electric vectors in the two cases.

Since  $\vec{J}_1$  and  $\vec{J}_2$  are assumed to vanish except in the vicinity of  $\vec{r}_1$  and  $\vec{r}_2$ ,  $\vec{E}_1$  and  $\vec{E}_2$  can be evaluated at these two points, reducing

(3.3-1) to

$$\vec{E}_1(\vec{r}_2) \cdot \iiint \vec{J}_2 dV = \vec{E}_2(\vec{r}_1) \cdot \iiint \vec{J}_1 dV \quad (3.3-2)$$

where the integrations are performed over the regions in which  $\vec{J}_1$  and  $\vec{J}_2$  do not vanish. Thus, if  $\vec{E}_1(\vec{r}_2)$  is known for arbitrary  $\iiint J_1 dV$  and if  $\vec{J}_2$  is specified, then  $\vec{E}_2(\vec{r}_1)$  can be calculated. It also follows from (3.3-2) that for smooth finite surfaces, the effective radar cross-section remains the same if the transmitter and receiver are interchanged.

When an approximation technique is used to obtain the cross-section, the foregoing reciprocity relationship may not hold. Therefore, the current-distribution method must be investigated to determine if reciprocity relations exist for it. According to the current-distribution method, the effective cross-section of a convex body is given by

$$\sigma_e(\beta) = \frac{4\pi}{\lambda^2} \left| (\hat{n}_o \cdot \hat{a})(\vec{f} \cdot \hat{d}) - (\hat{n}_o \cdot \vec{f})(\hat{a} \cdot \hat{d}) \right|^2 \tag{3.2-6}$$

where

$$\vec{f} = \int \hat{n} \exp [-ik\vec{r} \cdot (\hat{n}_o + \hat{k})] dS$$

illuminated  
portion of  
the surface

When the wavelength becomes extremely short, all the contributions to  $\vec{f}$  cancel out except those from the immediate vicinity of the stationary-phase point on the side of the body toward the transmitter. A stationary-phase point is one at which a plane of constant phase,  $(\hat{n}_o + \hat{k}) \cdot \vec{r} = \text{const.}$ , is tangent to the surface of the body. Clearly  $\hat{n} = (\hat{n}_o + \hat{k}) / |\hat{n}_o + \hat{k}|$  at a stationary-phase point, and for extremely short wavelengths  $\vec{f} = A(\hat{n}_o + \hat{k})$  where  $A$  is not changed by an interchange of transmitter

and receiver. Therefore, in this limiting case, (3.2-6) becomes

$$\sigma_e \approx \frac{4\pi}{\lambda^2} |A|^2 \left| (1 + \hat{n}_o \cdot \hat{k}) (\hat{a} \cdot \hat{d}) - (\hat{n}_o \cdot \hat{a}) (\hat{k} \cdot \hat{d}) \right|^2. \quad (3.3-3)$$

If  $\hat{n}_o$  and  $\hat{k}$  are interchanged, and simultaneously  $\hat{a}$  and  $\hat{d}$  are interchanged, (3.3-3) is unaffected. Hence, reciprocity is obtained for the current-distribution method in the limit of extremely short wavelengths. The same result would follow if the region of integration in the definition of  $\vec{f}$  were taken to be any region which enclosed the necessary stationary-phase point. For the convex bodies under consideration in this paper, the stationary-phase point lies in the region seen by both transmitter and receiver. An illustration of the difference between these two regions of integration is shown in Figure 4. The figure shows the projections of the shadow curves and of the regions of integration onto the yz-plane for each case; the transmitter is on the z-axis and a sphere is the surface used in this illustration.

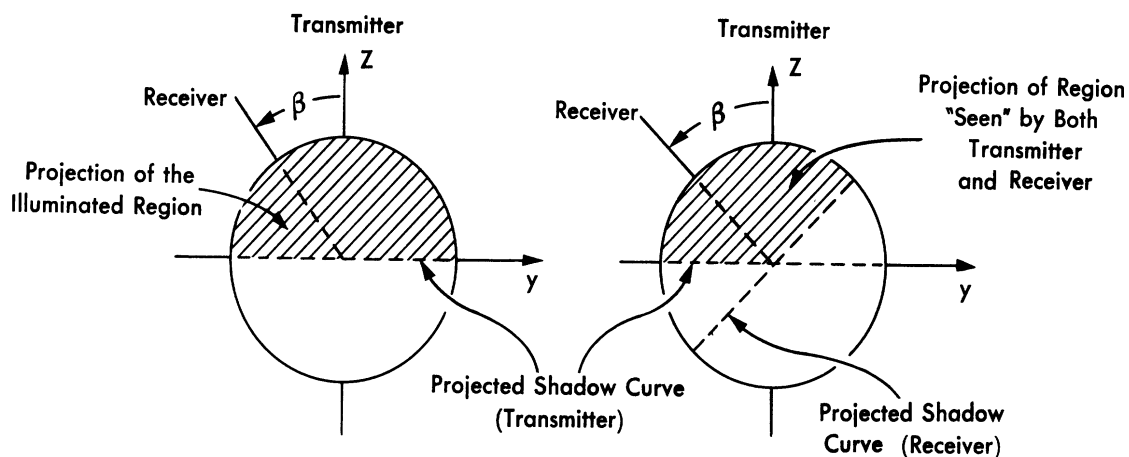


FIG. 4 PROJECTIONS OF SHADOW CURVES AND REGIONS OF INTEGRATION

When a wavelength-dependent expression for the cross-section is obtained by the current-distribution method, complete reciprocity is not obtained. At a casual glance it might appear that reciprocity could be regained by choosing the region of integration to be the part of the scatterer seen by both transmitter and receiver. Although the region of integration is already fixed in the current-distribution method, the new choice of the region of integration would be justified if it yielded correct results. As noted above the stationary-phase point is included in the new region of integration so that the correct effective cross-section is obtained in the limit as  $\lambda \rightarrow 0$ . Furthermore, the value of  $\vec{f}$  is not affected by an interchange of transmitter and receiver. However, this is not the condition for reciprocity. As can be seen from (3.2-6),  $\vec{f}$  is operated on in a fashion which is not symmetrical with respect to an interchange of transmitter and receiver. If (3.2-6) were to give reciprocity independently of the wavelength, it would have to give reciprocity even for very large wavelengths. Therefore, consider the following counter-example:

Let  $2\pi L/\lambda \ll 1$

where  $L$  is the maximum dimension of the body, then  $\vec{f} \approx \int \hat{n} dS$ .

Let  $\hat{k} = \hat{d}$  and  $\hat{n} = \hat{a} = \hat{i}_y$

and take a scattering body which is symmetrical with respect to the  $yz$ -plane.

Then  $\vec{f} = A_r \hat{i}_y + A_t \hat{i}_x$

where  $A_r$  and  $A_t$  are the projections of the region of integration in the direction of receiver and transmitter respectively. Hence,

$$\sigma_e = 4\pi \frac{A_t^2}{\lambda^2} .$$

Obviously, reciprocity does not hold unless  $A_r = A_t$ . In general this is not the case. For example, for receiver and transmitter nose-on and broadside, respectively, to a prolate spheroid,  $A_r \neq A_t$ , and hence reciprocity is not obtained by using this different region of integration.

If  $\sigma_0$  is the exact effective cross-section for a pair of reciprocal cases,  $\sigma_1$  and  $\sigma_2$  are the two approximations to the effective cross-section obtained by the current-distribution method,  $\sigma_1^*$  and  $\sigma_2^*$  are the two approximations to the effective cross-section obtained when the current-distribution method is modified so as to make the region of integration that part of the scatterer seen by both transmitter and receiver, then

- 1) As  $\lambda \rightarrow 0$  all of the values  $\sigma_1$ ,  $\sigma_2$ ,  $\sigma_1^*$ , and  $\sigma_2^*$  approach the value  $\sigma_0$ ,
  - 2) In general  $\sigma_1 \neq \sigma_2$  and  $\sigma_1^* \neq \sigma_2^*$ ,
- and 3) Only one integral need be evaluated to obtain  $\sigma_1^*$  and  $\sigma_2^*$  while two different integrals are needed for  $\sigma_1$  and  $\sigma_2$  (however, each of these will in some cases be simpler than the one required for  $\sigma_1^*$  and  $\sigma_2^*$  since the limits of integration are simpler).

$\sigma_1$  and  $\sigma_2$  are obtained by making physically reasonable assumptions while  $\sigma_1^*$  and  $\sigma_2^*$  have been obtained by making a further approximation. Thus it is to be expected that in most cases both  $\sigma_1$  and  $\sigma_2$  are better approximations to  $\sigma_0$  than either  $\sigma_1^*$  or  $\sigma_2^*$ . It is not necessary to calculate both  $\sigma_1$  and  $\sigma_2$ . Instead either  $\sigma_1$  or  $\sigma_2$  can be used as an approximation to  $\sigma_0$ .

It has been established that if the body is smooth and finite in size (e.g., sphere, spheroid), the reciprocity relationship holds for the geometric-optics approximation. Although reciprocity has not been established formally for semi-infinite or pointed bodies, experience in computing physical-optics cross-sections has shown that  $\sigma_1$  and  $\sigma_2$  agree fairly well with one another even for these bodies.

## IV

THE BISTATIC CROSS-SECTION OF FINITE SURFACES  
OF REVOLUTION WITH THE TRANSMITTER LOCATED  
ON THE AXIS OF SYMMETRY OF THE BODY

The bistatic radar cross-section of a prolate spheroid, a sphere, an ogive, and a finite cone have been determined under the following conditions: The transmitter is located on the z-axis, the direction of polarization at the transmitter,  $\hat{a}$ , is  $\hat{i}_y$ , and the geometry is that shown in Figure 3. Under these conditions, the radar cross-section is given by

$$\sigma_{\hat{a}=\hat{i}_y}^{\hat{z}}(\beta) = \frac{4\pi}{\lambda^2} |I_z|^2 \quad (3.2-8)$$

where  $I_z = \int_{\text{illuminated portion of surface}} n_z \exp[-ik\vec{r} \cdot (\hat{n}_o + \hat{k})] dS.$

$I_z$  has been evaluated both by the D.S.P. theorem (the details appear in Appendix 2) and on electronic analog computing equipment for the prolate spheroid, the sphere, and the ogive. By using both methods of evaluation, it is possible to compare the results obtained from geometric optics (D.S.P. theorem in the limit as  $\lambda$  tends to zero) with those obtained from physical optics (analog computer). The analog computing equipment consisted of standard Reeves Analog Computer units and the evaluation was carried out by analytical integration in one variable and electronic integration in the other.\*

\*The details involved in evaluating these integrals on analog equipment were presented in a paper, "Use of the Analog Computer in Evaluating Integrals of the Form  $\int_0^\phi \sin\theta \cos\theta J_0(A \sin\theta) e^{iC \cos\theta} d\theta$ ," by E. C. Licht and V. L. Larowe at the October 14, 1953 meeting of the Project TYPHOON Symposium III, at the University of Pennsylvania.

4.1: The Prolate Spheroid

In prolate spheroidal coordinates,\* the integral  $I_z$  for a prolate spheroid  $\frac{x^2 + y^2}{B^2} + \frac{z^2}{A^2} = 1$  is expressed as

$$I_z = B^2 \int_0^1 \int_0^{2\pi} \eta \exp \left[ -i \left\{ a\sqrt{1-\eta^2} \sin\phi - b\eta \right\} \right] d\phi d\eta \quad (4.1-1)$$

where  $a = kB \sin \beta$  and  $b = kA(1 + \cos \beta)$ .

Since (Ref. 15, p. 26)

$$\int_0^{2\pi} \exp [-ik\psi \sin\phi] d\phi = 2\pi J_0(k\psi), \quad (4.1-2)$$

$I_z$  can be expressed in the form

$$I_z = 2\pi B^2 \int_0^{\pi/2} \sin\theta \cos\theta J_0(a \sin\theta) e^{ib \cos\theta} d\theta \quad (4.1-3)$$

\*The relations between the prolate spheroidal coordinates and the rectangular are given by

$$x = c \sqrt{(1-\eta^2)(\xi^2-1)} \cos\phi$$

$$y = c \sqrt{(1-\eta^2)(\xi^2-1)} \sin\phi$$

$$z = c \eta$$

$$\xi = \xi_0$$

defines a prolate spheroid of rotation around the z-axis with the rectangular form

$$\frac{x^2 + y^2}{c^2(\xi_0^2 - 1)} + \frac{z^2}{c^2 \xi_0^2} = 1$$

Thus, from (3.2-8)

$$\frac{\sigma_{a=i}^{\wedge \wedge}(\beta)}{\left\{ \pi B^4 / A^2 \right\}} = \left( \frac{kA}{\pi} \right)^2 \left| 2\pi \int_0^{\pi/2} \sin\theta \cos\theta J_0(a \sin\theta) e^{ib \cos\theta} d\theta \right|^2. \quad (4.1-4)$$

Equation (4.1-4) has been evaluated on analog computing equipment for two cases:  $A = 10B$  and  $kB = 100$ , and  $A = 10B$  and  $kB = 5$ . The results of these evaluations are shown in Figure 5.

$\sigma_{a=i}^{\wedge \wedge}(\beta)$  can be approximated by applying the D.S.P. theorem.

The application of this theorem yields the "geometric-optics" result:

$$\frac{\sigma_{a=i}^{\wedge \wedge}(\beta)}{\left\{ \pi B^4 / A^2 \right\}} \approx \frac{4}{\left[ (1 + \cos\beta) + \frac{B^2}{A^2} (1 - \cos\beta) \right]^2}, \quad \beta < \pi. \quad (4.1-5)$$

Equation (4.1-5) is also shown on Figure 5. Examination of this figure shows that for  $0^\circ \leq \beta < 160^\circ$  the analytic curve representing (4.1-5) appears to be a good approximation to the analog evaluation for values of  $kB$  which are greater than or equal to 5.

#### 4.2: The Sphere

$I_z$  for a sphere of radius  $R_0$  is given by (4.1-1) with  $A = B = R_0$ , and  $\sigma(\beta) / \pi R_0^2$  for the sphere is given by (4.1-4) with  $A = B = R_0$ . Equation (4.1-4) with both  $A$  and  $B$  replaced by  $R_0$  has been evaluated on analog equipment for the cases  $kR_0 = 100$  and  $kR_0 = 5$ . The results of these evaluations and the geometric-optics result ( $\sigma = \pi R_0^2$ ) are shown in Figure 6. As in the case of the prolate spheroid, the



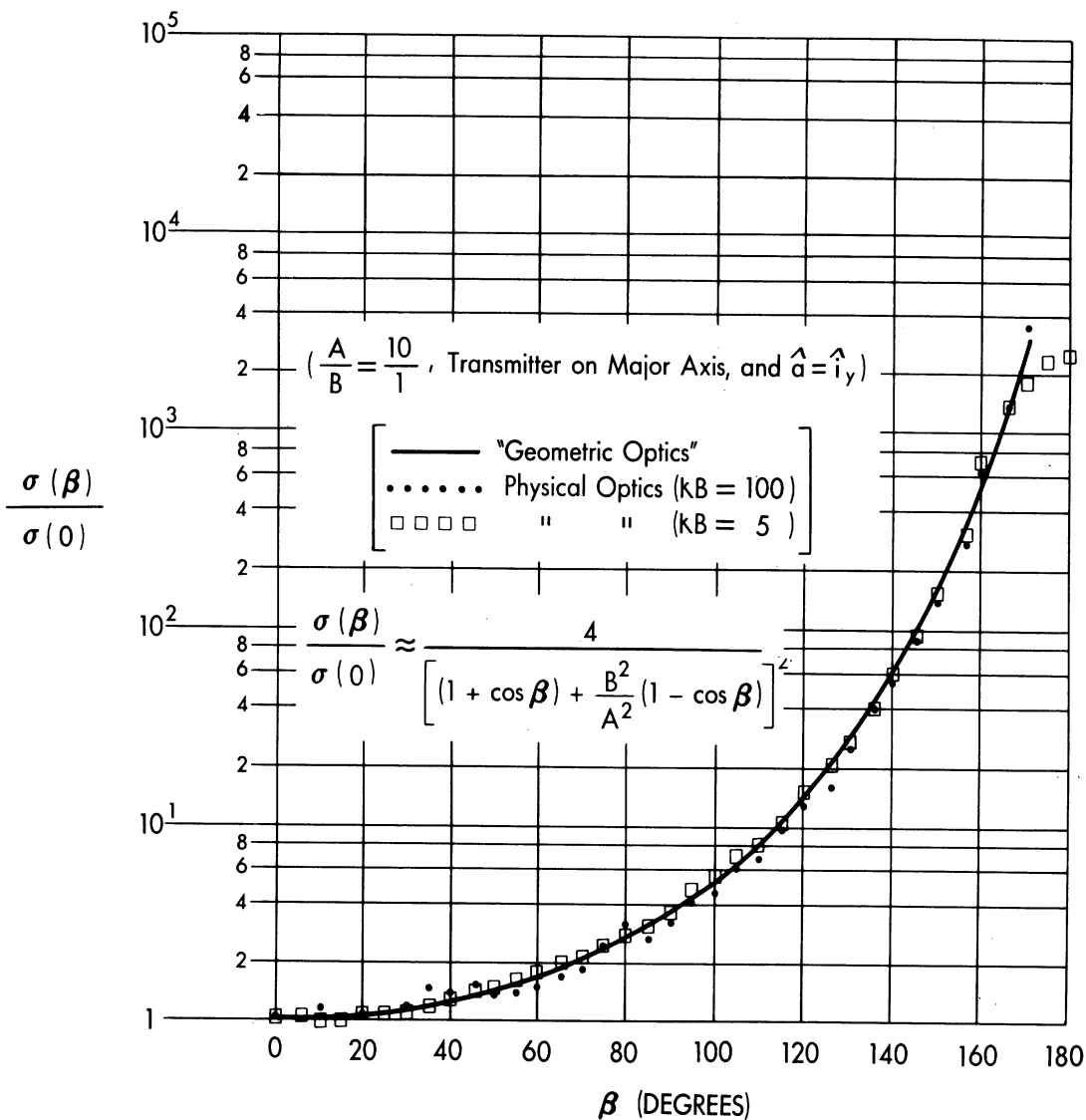


FIG. 5 CROSS-SECTION OF A PROLATE SPHEROID AS A FUNCTION OF  $\beta$

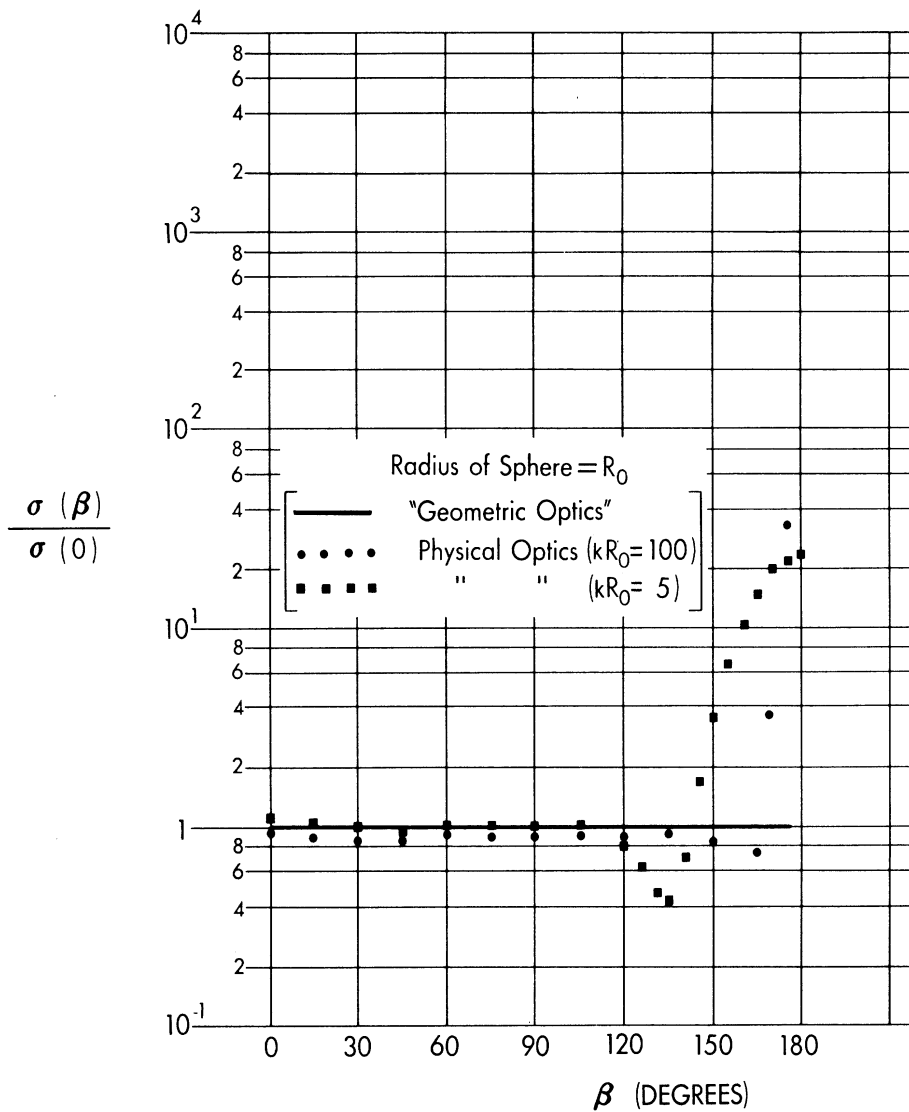


FIG. 6 CROSS-SECTION OF A SPHERE AS A FUNCTION OF  $\beta$

geometric-optics result obtained by using the D.S.P. theorem agrees closely with the physical-optics result in the range of  $0^\circ \leq \beta < 120^\circ$ .

4.3: The Ogive

The term "ogive" is not defined uniformly in the literature. For example, Hobson (Ref. 16, p. 451) refers to the figure obtained by revolving a minor arc of a circle around its chord as a spindle whereas Hansen and Schiff (Ref. 17) use the term spindle to describe the arc of a parabola revolved around its chord. Others use the term ogive as a general term of which both of the above configurations are examples. In the work presented here the term ogive refers to the minor arc of a circle revolved around its chord (Hobson's spindle) and the term spindle will be used for the parabolic arc revolved around its chord (Hansen and Schiff).

An ogive of length  $L$ , maximum diameter  $d$ , and half-angle  $\alpha$  (using the cylindrical coordinates  $(w, \phi, z)$ ) is given by the equation

$$(w + h)^2 + z^2 - p^2 = 0 \tag{4.3-1}$$

with  $|z| \leq \sqrt{p^2 - h^2} = L/2$ ,

$$h \leq w + h \leq p,$$

and  $\alpha = \cos^{-1}(h/p)$ .

These relations are shown in Figure 7.

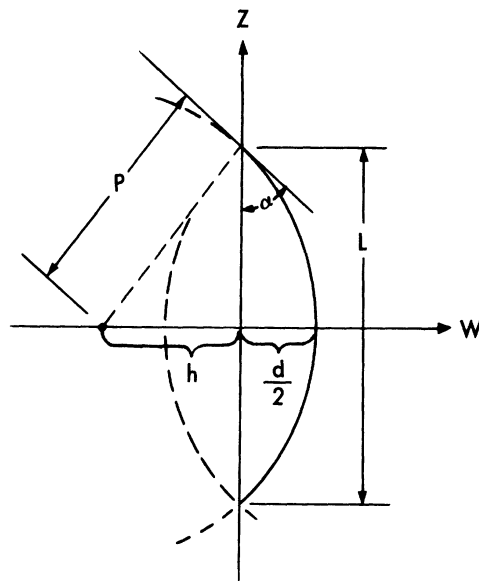


FIG. 7 GEOMETRY FOR THE OGIIVE

The integral  $I_z$  takes on the form

$$I_z = \int_0^{p-h} \int_0^{2\pi} w e^{ikf(w)} e^{-ikw \sin \beta \sin \phi} d\phi dw \quad (4.3-2)$$

where  $f(w) = (1 + \cos \beta) \sqrt{p^2 - (w+h)^2}$  .

The application of the D.S.P. theorem to (4.3-2) yields

$$\sigma_{\hat{a}=\hat{i}_y}^{\hat{a}=\hat{i}_y}(\beta) = \frac{\pi L^2 \left\{ \sin(\beta/2) - \cos \alpha \right\}}{4 \sin^2 \alpha \sin(\beta/2)} \quad \pi - 2\alpha < \beta < \pi. \quad (4.3-3)$$

The theorem implies that in the range  $0 \leq \beta \leq \pi - 2\alpha$ ,  $\sigma(\beta) = 0$  in the limit of vanishing wavelength (See Appendix 2). To obtain information about  $\sigma(\beta)$  in the range  $0 \leq \beta \leq \pi - 2\alpha$ , first apply (4.1-2) to (4.3-2) obtaining

$$I_z = 2\pi p^2 \int_0^\alpha (\cos \theta - \cos \alpha) \sin \theta J_0(a[\cos \theta - \cos \alpha]) e^{ib \sin \theta} d\theta \quad (4.3-4)$$

where  $a = kp \sin \beta$ ,  $b = kp(1 + \cos \beta)$ , and the transformation defined by  $w + h = p \cos \theta$  has been employed.

In obtaining information relative to  $\sigma(\beta)$  in the range  $0 \leq \beta \leq \pi - 2\alpha$ , first consider the left end of the interval, the case of back-scattering. For  $\beta = 0$  (4.3-4) reduces to

$$I_z = 2\pi p^2 \int_0^\alpha (\cos \theta - \cos \alpha) \sin \theta e^{ib_0 \sin \theta} d\theta \quad (4.3-5)$$

where  $b_0 = b_{(\beta=0)} = 2kp = 4\pi p/\lambda$ .

This integral can be evaluated by parts to yield

$$I_z = \frac{2\pi p^2}{(ib_0)^2} \left[ \tan^2 \alpha e^{ib_0 \sin \alpha} + (1 - \cos \alpha) \right] + O\left(\frac{1}{(ib_0)^3}\right), \quad (4.3-6)$$

if  $\sqrt{\lambda/4\pi p} < \alpha < \frac{\pi}{2} - \sqrt{\lambda/4\pi p}$ .

Use of (4.3-6) would imply that the contributions from the tip of the ogive and from the shadow rim ( $z = 0, w = p - h$ ) are of the same order of magnitude.\* Hansen and Schiff, who obtained a similar result in their

\*Use of the evaluation of  $I_z$  given in (4.3-6) yields the cross-section formula

$$\sigma(0) = \frac{\lambda^2 \tan^4 \alpha}{16\pi} \left[ 1 + \frac{2 \cos^2 \alpha \cos\left(\frac{2\pi L}{\lambda}\right)}{1 + \cos \alpha} + \frac{\cos^4 \alpha}{(1 + \cos \alpha)^2} \right].$$

work on the spindle (Ref. 17), showed by a more careful consideration of the contribution of the shadow rim that, in fact, the contribution of the shadow rim (or rather, the penumbra) is of a smaller order of magnitude than that of the point and that the "correct" answer can be obtained by merely evaluating the integral at the "tip". Their analysis of the penumbra region, which is also valid for the ogive, is discussed in more detail in Appendix 3.

By applying Hansen and Schiff's penumbra analysis to the ogive problem, i.e., ignoring the contribution from the shadow rim ( $w = p - h$ , or  $\theta = 0$ ) it is found that  $\sigma(0)$  for the ogive is given by

$$\sigma(0) = \frac{\lambda^2 \tan^4 \alpha}{16\pi}, \quad \sqrt{1/b_0} < \alpha < \frac{\pi}{2} - \sqrt{1/b_0}. \quad (4.3-7)$$

The nature of  $\sigma(\beta)$  in the region  $0 < \beta < \pi - 2\alpha$  has still to be determined. Assuming that the tip will also dominate for most of the values of  $\beta$  in this region (i.e., for  $0 < \beta < \pi - 2\alpha - |\beta_0(\lambda)|$  where  $\beta_0(\lambda) \rightarrow 0$  as  $\lambda \rightarrow 0$ ) as it did for  $\beta = 0$  and using an approach similar to that employed in obtaining (4.3-7) the tip formula for the ogive becomes\*

$$\sigma_{\hat{a}=1}^{\hat{y}}(\beta) = \frac{\lambda^2 \tan^4 \alpha}{16\pi} \frac{(1 - \tan^2 \alpha \tan^2(\beta/2))^{-3}}{\cos^8(\beta/2)}. \quad (4.3-8)$$

It is obvious that for small  $\alpha$  and for  $\beta < \pi/2$  equation (4.3-8) may be approximated by

$$\sigma_{\hat{a}=1}^{\hat{y}}(\beta) = \frac{\lambda^2 \tan^4 \alpha}{16\pi} \sec^8(\beta/2). \quad (4.3-9)$$

---

\*It may be readily observed that this formula is identically the same as that obtained for the semi-infinite cone (Sec. 5.2).

The analysis presented above, which presents a tip formula for the cross-section in the range  $0 \leq \beta < \pi - 2\alpha$  and a geometric-optics formula in the range  $\pi - 2\alpha < \beta < \pi$ , does not give information about the cross-section at or in the immediate vicinity of  $\beta = \pi - 2\alpha$ . For a particular choice of  $L$  and  $\lambda$ , the cross-section in this transition region can be estimated either by a curve-fitting process or by applying analog computing methods to the integral (4.3-4).

$\sigma(\beta)$  was evaluated on analog equipment for the case defined by  $\alpha = 15^\circ$  and  $\pi d/\lambda = 100$  using Equation (4.3-4). The nature of the integrand made it difficult to obtain reliable results over the entire range in  $\beta$ ; however, fairly reliable results were obtained in the interval  $\frac{\pi}{2} < \beta < \pi$ .

A plot of the ratio  $\sigma(\beta)/\sigma(0)$  determined both from (4.3-8) and from (4.3-9) appears in Figure 8 for  $0 \leq \beta < 140^\circ$ . The analog evaluations are included for comparison.

Figure 9 is a graph of the results obtained by

- (1) the "tip" method of determination (Eqns. (4.3-8) and (4.3-9)),
- (2) the analog evaluation (reliable for  $\beta > \pi/2$ ), and
- (3) the D.S.P. result (Eqn. 4.3-3), valid for  $\pi - 2\alpha < \beta < \pi$ , for the special case defined by  $\alpha = 15^\circ$  and  $\pi d/\lambda = 100$ . The figure displays a plot of  $\sigma(\beta)/\lambda^2$  vs  $\beta$  for  $0 \leq \beta \leq \pi$ . Examination of this figure seems to indicate that if a single curve were to be fitted through this data, it would follow the "tip" formula almost up to the  $\pi - 2\alpha$  value of  $150^\circ$  and then follow the trend indicated by the analog evaluations and the D.S.P. result. It may be observed that the analog evaluations and the D.S.P. result are in close agreement in the range  $155^\circ < \beta < 175^\circ$ .

UMM-115

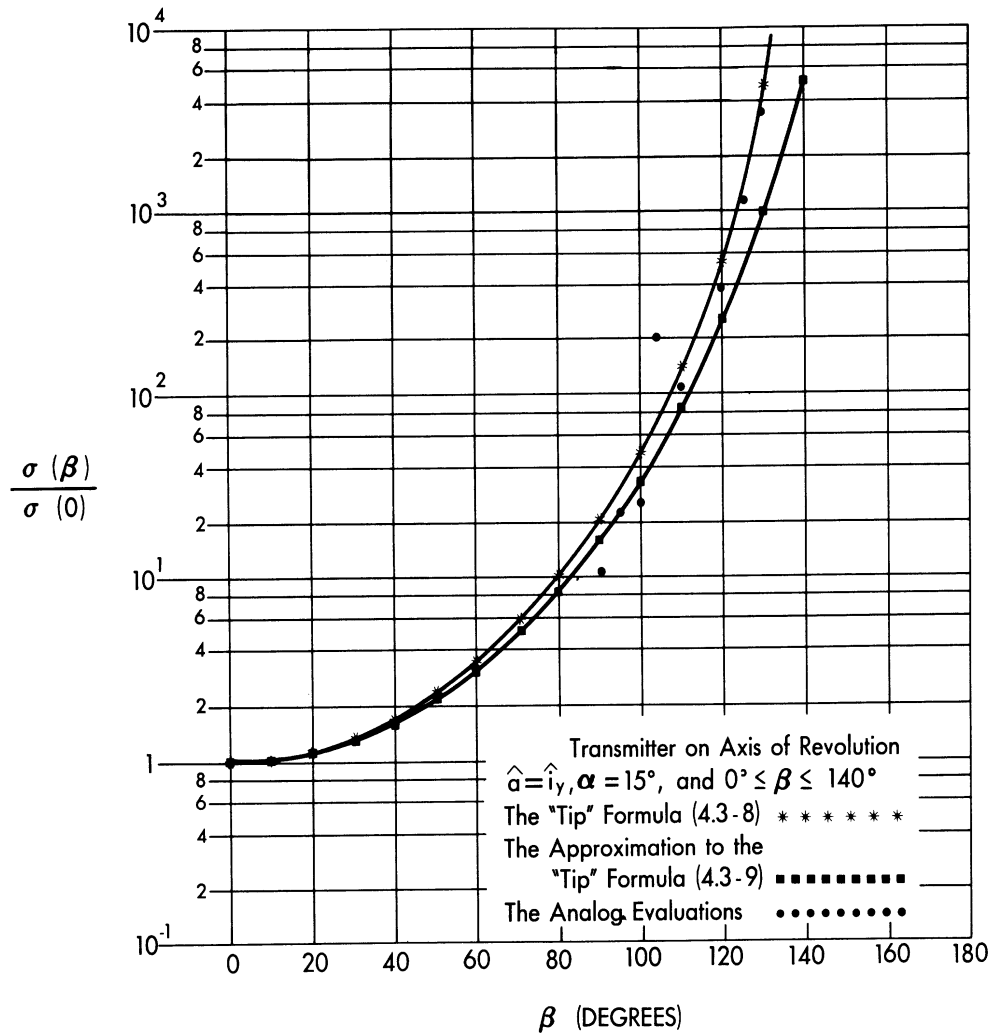


FIG. 8 CROSS-SECTION OF AN OGIVE OF HALF-ANGLE  $\alpha$  AND LENGTH L AS A FUNCTION OF  $\beta$



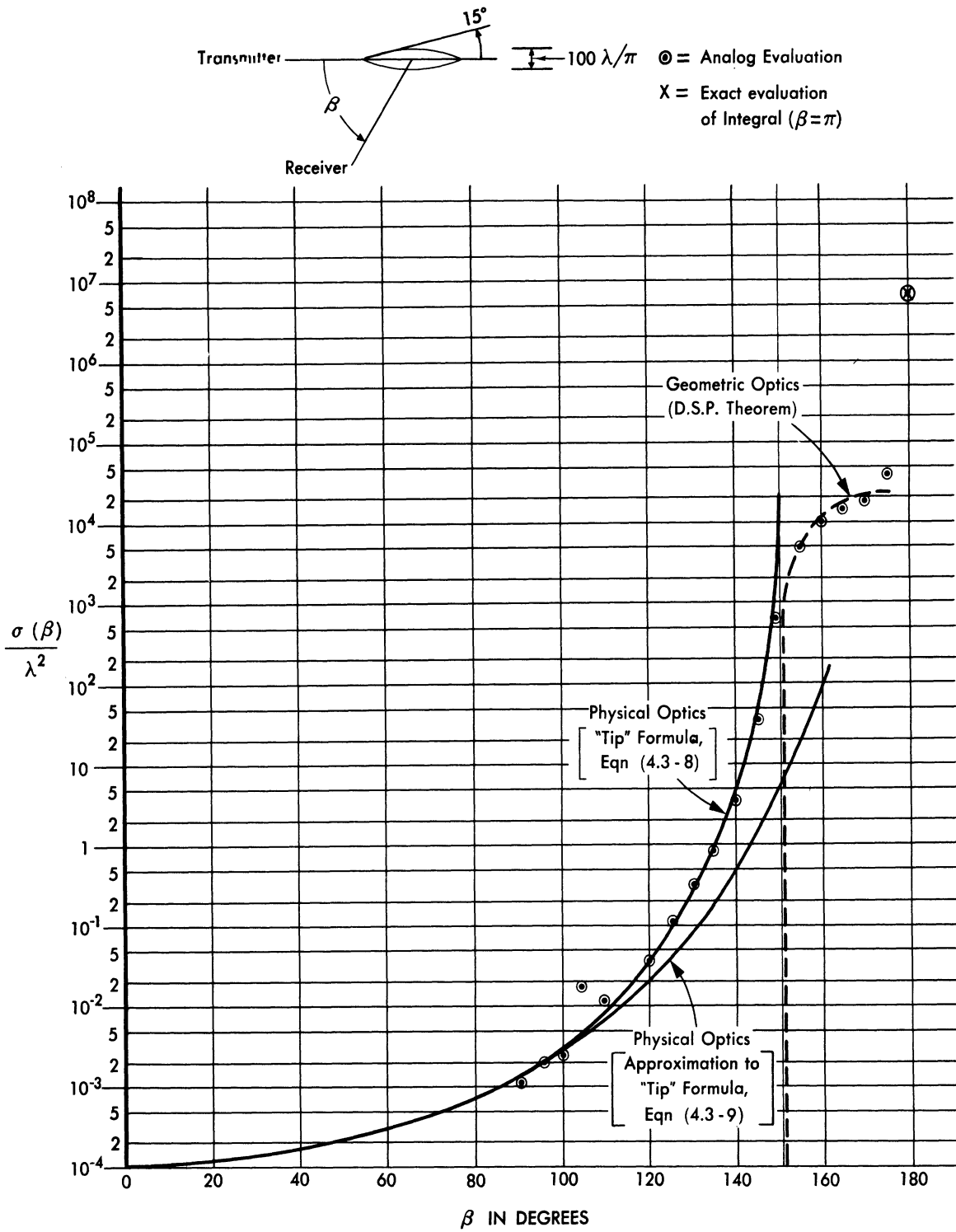


FIG. 9 CROSS-SECTION OF AN OGIVE OF HALF-ANGLE  $15^\circ$  AND MAXIMUM DIAMETER EQUAL TO  $100 \lambda/\pi$

4.4: The Finite Cone

For the finite cone,  $I_z$  is expressed in spherical coordinates as

$$I_z = \sin^2 \gamma \int_0^{2\pi} \int_0^{r_0} r e^{-ikrg(\phi)} dr d\phi \quad (4.4-1)$$

where  $g(\phi) = \sin \gamma \sin \beta \sin \phi + (1 + \cos \beta) \cos \gamma$  and  $\gamma = 1/2$  the cone angle.

Upon integration by parts, (4.4-1) becomes

$$I_z = \sin^2 \gamma \int_0^{2\pi} \left[ \frac{e^{-ikg(\phi)r_0}}{[-ikg(\phi)]^2} \left\{ -ikr_0 g(\phi) - 1 \right\} + \frac{1}{[-ikg(\phi)]^2} \right] d\phi \quad (4.4-2)$$

which may be written in the form

$$I_z = \sin^2 \gamma \left[ \frac{ir_0}{k} \int_0^{2\pi} \frac{e^{-ikr_0(b \sin \phi + c)}}{(b \sin \phi + c)} d\phi + \frac{1}{k^2} \int_0^{2\pi} \frac{e^{-ikr_0(b \sin \phi + c)}}{(b \sin \phi + c)^2} d\phi - \frac{1}{k^2} \int_0^{2\pi} \frac{d\phi}{(b \sin \phi + c)^2} \right] \quad (4.4-3)*$$

with  $b = \sin \beta \sin \gamma$  and  $c = \cos \gamma (1 + \cos \beta)$ .

---

\*The quantity  $(b \sin \phi + c)$  remains non-zero (and positive) for  $0 \leq \phi \leq 2\pi$  if  $0 \leq \beta < \pi - 2\gamma$ .

For  $\beta = 0$ , the above expression for  $I_z$  yields

$$\sigma_{a=i}^{\wedge \wedge} (0) \approx \frac{\pi r_o^2 \sin^4 \gamma}{\cos^2 \gamma}. \quad (4.4-4)$$

If  $\beta$  is bounded away from zero and (4.4-3) is evaluated by the methods of stationary phase, the first of the three integrals in (4.4-3) dominates and hence

$$I_z = (\sin^2 \gamma) \frac{ir_o}{k} \int_0^{2\pi} \frac{e^{-ikr_o(b \sin \phi + c)}}{(b \sin \phi + c)} d\phi$$

$$\approx \frac{-2i\pi r_o \sin^2 \gamma}{k(b^2 - c^2)} e^{-ikr_o c} \left[ \frac{c \cos(kr_o b - \frac{\pi}{4}) + ib \sin(kr_o b - \frac{\pi}{4})}{\left(\frac{\pi kr_o b}{2}\right)^{1/2}} \right]. \quad (4.4-5)$$

If  $kr_o \gg 1$ , the expressions inside the brackets of Equation (4.4-5) can be replaced by their equivalent asymptotic forms. Thus (4.4-5) takes on the form

$$I_z = \frac{-2i\pi r_o \sin^2 \gamma}{k(b^2 - c^2)} e^{-ikr_o c} \left[ c J_0(kr_o b) + ib J_1(kr_o b) \right], \quad (4.4-6)$$

from which it follows that

$$\sigma_{\frac{\hat{a}=1}{\hat{y}}}^{\hat{\alpha}}(\beta) = \frac{4\pi r_o^2 \sin^4 \gamma}{(b^2 - c^2)^2} \left[ c^2 \left\{ J_o(kr_o b) \right\}^2 + b^2 \left\{ J_1(kr_o b) \right\}^2 \right]. \quad (4.4-7)$$

Although (4.4-7) was derived under the assumption that  $\beta > 0$ , it reduces to (4.4-4) if  $\beta = 0$ .

The bistatic cross-section of the finite cone is shown in Figure 10. The curve is drawn for the special case defined by  $\gamma = 15^\circ$  and  $\pi r_o / \lambda = 100$ .

It should be pointed out that the sharp edge of the finite cone contradicts the assumptions of the current-distribution method. Thus, the result obtained here for the finite cone may not be as good an approximation to the exact cross-section as the results obtained for other bodies.

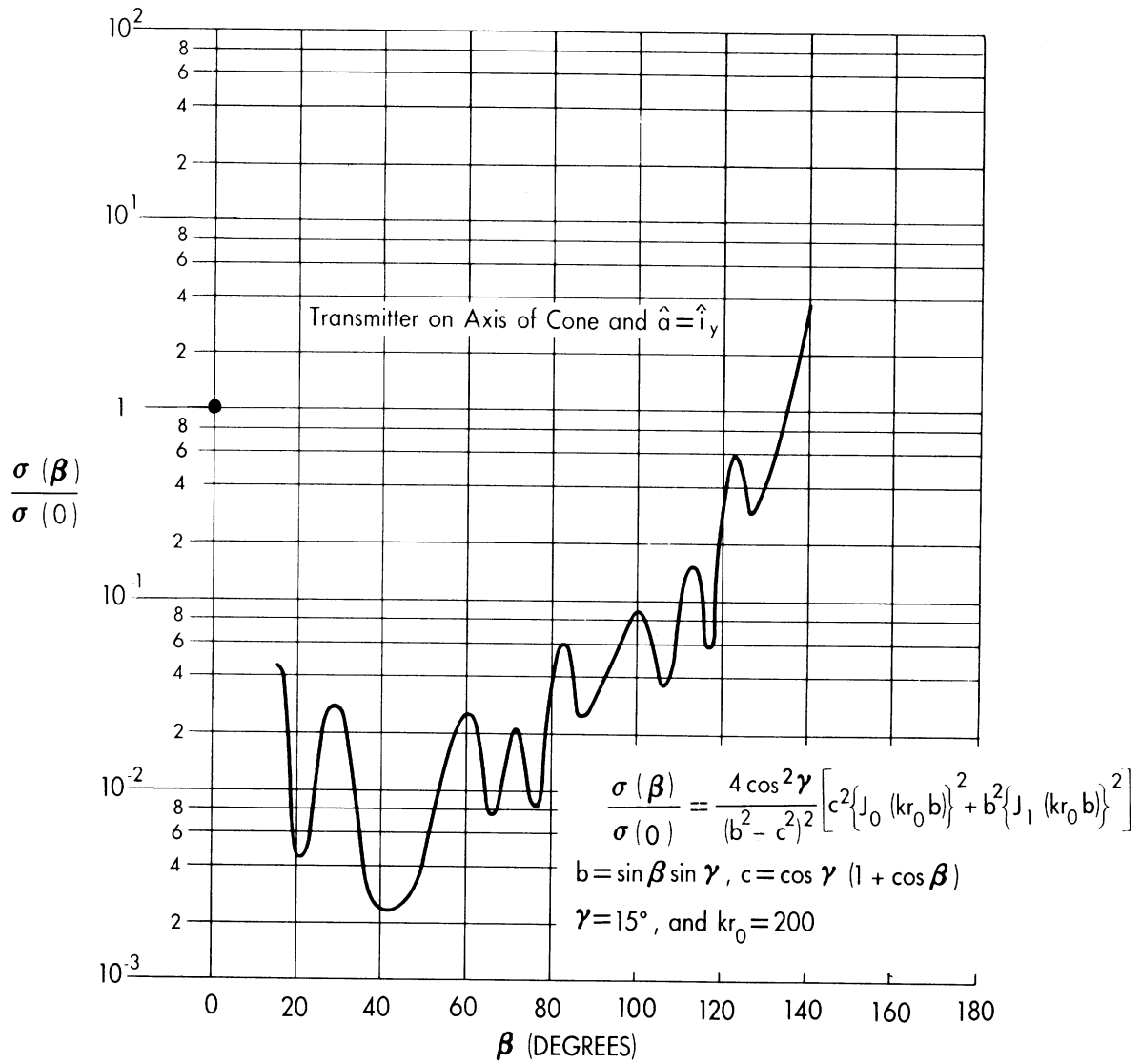


FIG. 10 CROSS-SECTION OF A FINITE CONE OF HALF-ANGLE  $\gamma$

## V

THE BISTATIC CROSS-SECTION OF SEMI-INFINITE  
SURFACES OF REVOLUTION WITH THE TRANSMITTER  
LOCATED ON THE AXIS OF SYMMETRY

Although the current-distribution method employed in this paper is based on the assumption that the surface is finite (Section 3.2), this method can be applied to determine  $\sigma_{\hat{a}=\hat{y}}(\beta)$  for the paraboloid and for the semi-infinite cone (if the integral is evaluated with the aid of an Abelian limit process). The results obtained in this way have been checked by comparing them with the known result for  $\beta = 0$  and with the answers obtained from the Luneberg-Kline method (Ref. 18). The details involved in applying the Luneberg-Kline method to this problem appear in Appendix 4.

## 5.1: The Paraboloid

For the paraboloid defined by the equation  $r^2 = -4pz$  (using the system configuration shown in Figure 3),

$$I_z = \int_0^\infty \int_0^{2\pi} r \exp \left\{ -i \left[ ar \sin \phi + br^2 \right] \right\} d\phi dr \quad (5.1-1)$$

where  $a = k \sin \beta$  and  $b = k(1 + \cos \beta)/4p$ .

Using the relation (4.1-2)

$$I_z = 2\pi \int_0^\infty r \exp \left[ -ibr^2 \right] J_0(ar) dr \quad (5.1-2)$$

$$\begin{aligned}
 &= \pi \int_0^{\infty} J_0(a\sqrt{u}) e^{-ibu} du \\
 &= \frac{\pi}{ib} \exp(ia^2/4b), \qquad \text{(Ref. 19, p. 80).}
 \end{aligned}$$

Thus  $|I_z|^2 = 4 p^2 \lambda^2 / (1 + \cos \beta)^2$  and therefore the use of the relation (3.2-8) yields

$$\sigma_{a=i_y}^{\wedge}(\beta) = 16\pi p^2 / (1 + \cos \beta)^2. \qquad (5.1-3)$$

As shown in Appendix 4, the geometric-optics answer is the exact solution to axially symmetric scattering from the paraboloid of revolution; that is, (5.1-3) gives the exact cross-section of the paraboloid.

The bistatic cross-section,  $\sigma_{a=i_y}^{\wedge}(\beta)$ , of the paraboloid is shown as a function of  $\beta$  in Figure 11.

### 5.2: The Semi-Infinite Cone

The computation of the bistatic cross-section of a semi-infinite cone, which is carried out in this section, is restricted to the case in which the entire surface of the cone is illuminated. That is, if  $\gamma$  equals 1/2 the cone angle,  $\hat{k}_1$  denotes the transmitter direction, and  $\hat{c}$  the direction of the cone axis, the allowable range of  $\gamma$  is obtained from the relation

$$\left| \hat{k}_1 \cdot \hat{c} \right| \leq \cos \gamma. \qquad (5.2-1)$$

If  $\hat{n}_0'$  is the receiver direction, the geometry is that shown in Figure 12.

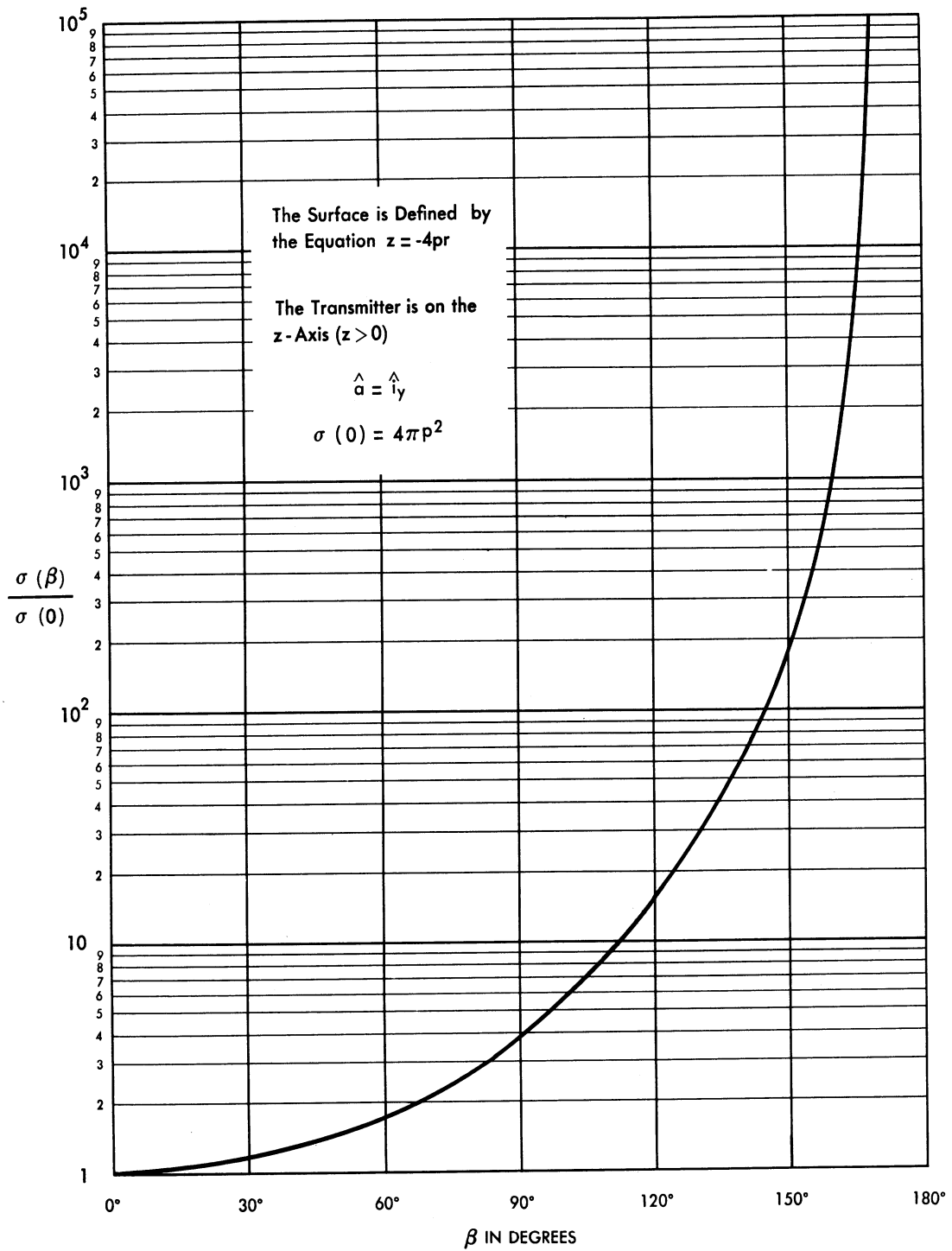


FIG. 11 THE BISTATIC CROSS-SECTION OF A PARABOLOID



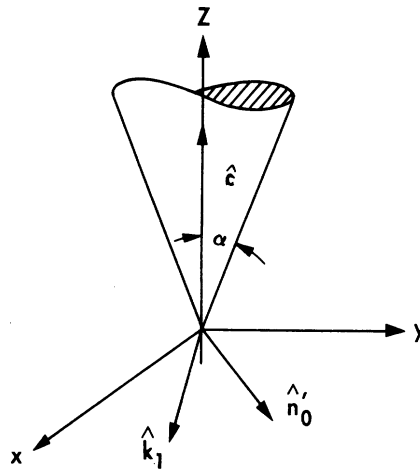


FIG. 12 GEOMETRY FOR SEMI-INFINITE CONE

The maximum possible cross-section of a body can be written as (Sec. 3.2)

$$\frac{4\pi}{\lambda^2} \left\{ |g_x|^2 + |g_y|^2 + |g_z|^2 \right\} \tag{5.2-2}$$

where  $g_x$ ,  $g_y$ , and  $g_z$  are the x, y, and z components of the vector

$$\vec{g} = (\hat{n}_0 \cdot \hat{a})\vec{f} - (\hat{n}_0 \cdot \vec{f})\hat{a}$$

and

$$\vec{f} = \int_{\substack{\text{surface} \\ \text{of cone}}} \exp \left[ ik\vec{r} \cdot (\hat{n}_0 + \hat{k}_1) \right] \hat{n} ds$$

$\hat{a}$  is the polarization of the incident wave,  $\hat{n}$  the normal to the cone, and

$$\vec{r} = \hat{i}_x x + \hat{i}_y y + \hat{i}_z z.$$

The integral  $\vec{f}$  can be expressed in the form

$$\int_{\text{surface of cone}} \left\{ \hat{i}_x (\hat{n} \cdot \hat{i}_x) + \hat{i}_y (\hat{n} \cdot \hat{i}_y) + \hat{i}_z (\hat{n} \cdot \hat{i}_z) \right\} e^{ik\vec{r} \cdot (\hat{n}_0' + \hat{k}_1)} ds$$

which in turn can be expressed in the equivalent form

$$\begin{aligned} & \hat{i}_x \int_{V'} \nabla \cdot \left[ \hat{i}_x e^{ik\vec{r} \cdot (\hat{n}_0' + \hat{k}_1)} \right] dV + \hat{i}_y \int_{V'} \nabla \cdot \left[ \hat{i}_y e^{ik\vec{r} \cdot (\hat{n}_0' + \hat{k}_1)} \right] dV \\ & + \hat{i}_z \int_{V'} \nabla \cdot \left[ \hat{i}_z e^{ik\vec{r} \cdot (\hat{n}_0' + \hat{k}_1)} \right] dV = ik(\hat{n}_0' + \hat{k}_1) \int_{V'} e^{ik\vec{r} \cdot (\hat{n}_0' + \hat{k}_1)} dV \end{aligned} \tag{5.2-3}$$

where  $V'$  = the volume enclosed by the surface. This integral can be converted to an integral over a single variable, namely the distance,  $\rho$ , measured from the origin, perpendicular to the constant phase fronts  $\vec{r} \cdot (\hat{n}_0' + \hat{k}_1) = |\hat{n}_0' + \hat{k}_1| \rho$ .  $dV$  is expressed in terms of  $d\rho$  as

$$dV = \frac{\pi \tan^2 \gamma}{\cos^3 \theta' [1 - \tan^2 \gamma \tan^2 \theta']^{3/2}} \rho^2 d\rho$$

where  $\theta' = \cos^{-1} \left\{ \frac{(\hat{k}_1 + \hat{n}_0') \cdot \hat{c}}{|\hat{k}_1 + \hat{n}_0'|} \right\}$ .

For simplicity, denote  $\frac{\pi \tan^2 \gamma}{\cos^3 \theta' [1 - \tan^2 \gamma \tan^2 \theta']^{3/2}}$  by  $\alpha'$ .

Then (5.2-3) takes on the form

$$ik(\hat{n}_0' + \hat{k}_1) \int_0^{\infty} a' e^{ik|\hat{n}_0' + \hat{k}_1|\rho} \rho^2 d\rho. \quad (5.2-4)$$

This integral is not convergent as it stands. To evaluate it, consider the Abelian limit as  $\delta \rightarrow 0$  of

$$\int_0^{\infty} a' e^{-\delta\rho} \exp\{ik|\hat{n}_0' + \hat{k}_1|\rho\} \rho^2 d\rho.$$

Let  $(\delta - ik|\hat{n}_0' + \hat{k}_1|)\rho = s$ ; then

$$\begin{aligned} & \lim_{\delta \rightarrow 0} \int_0^{\infty} a' \exp\{ik|\hat{n}_0' + \hat{k}_1|\rho - \delta\rho\} \rho^2 d\rho \\ &= \lim_{\delta \rightarrow 0} \frac{a'}{\{\delta - ik|\hat{n}_0' + \hat{k}_1|\}^3} \int_0^{\infty} e^{-s} s^2 ds \\ &= \frac{-2 a'}{(ik)^3 |\hat{n}_0' + \hat{k}_1|^3}. \end{aligned} \quad (5.2-5)$$

The components  $g_x$ ,  $g_y$ , and  $g_z$  can be computed with the aid of the expression in (5.2-5) e.g.,

$$\begin{aligned} \vec{g} &= (\hat{n}_0' \cdot \hat{a}) \left[ \frac{-2 a' ik(\hat{n}_0' + \hat{k}_1)}{(ik)^3 |\hat{n}_0' + \hat{k}_1|^3} \right] + \frac{2 a' ik [1 + \hat{n}_0' \cdot \hat{k}_1]}{(ik)^3 |\hat{n}_0' + \hat{k}_1|^3} \hat{a} \\ &= \frac{2 a' [-(\hat{n}_0' \cdot \hat{a})(\hat{n}_0' + \hat{k}_1) + (1 + \hat{n}_0' \cdot \hat{k}_1) \hat{a}] ik}{(ik)^3 |\hat{n}_0' + \hat{k}_1|^3}. \end{aligned}$$

Therefore,

$$|g_x|^2 + |g_y|^2 + |g_z|^2 = \frac{4 a'^2 [1 + \hat{k}_1 \cdot \hat{n}_{O'}]^2}{k^4 |\hat{n}_{O'} + \hat{k}_1|^6}, \quad (5.2-6)$$

and

$$\sigma = \frac{\lambda^2 \tan^4 \gamma [1 + \hat{k}_1 \cdot \hat{n}_{O'}]^2}{\pi |\hat{n}_{O'} + \hat{k}_1|^6 \cos^6 \theta' [1 - \tan^2 \gamma \tan^2 \theta']^3} \quad (5.2-7)$$

where

$\gamma$  = 1/2 the cone angle,

$\hat{k}_1$  is the transmitter direction (from target to transmitter),

$\hat{n}_{O'}$  is the receiver direction (from target to receiver),

$$\theta' = \cos^{-1} \left[ \frac{\hat{c} \cdot (\hat{k}_1 + \hat{n}_{O'})}{|\hat{k}_1 + \hat{n}_{O'}|} \right], \quad \text{and}$$

$\hat{c}$  is the direction of the cone axis.

If the notation is changed slightly to agree with that used in previous work, i.e.,

$$\hat{k}_1 = +\hat{i}_z$$

$$\hat{c} = -\hat{i}_z$$

$$\hat{n}_{O'} = -\hat{i}_y \sin \beta + \hat{i}_z \cos \beta,$$

then Equation (5.2-7) can be expressed in the form

$$\sigma(\beta) = \frac{\lambda^2 \tan^4 \gamma}{16\pi} \cdot \frac{2(1 + \cos 2\gamma)^3}{(1 + \cos \beta)(\cos \beta + \cos 2\gamma)^3} \quad (5.2-8)$$

Since the radius of curvature at the nose of the cone is zero, the Luneberg-Kline method cannot legitimately be applied to the cone problem. However, if the method is applied formally, the expression obtained (Eq. 5.2-9) has (5.2-8) as its first term. The Luneberg-Kline answer agrees with the intuitive expectation that the cross-section should be a maximum in the plane of electric polarization and a minimum in the plane of magnetic polarization. Also, the cross-section obtained by the formal application of the Luneberg-Kline method increases as a function of the separation between transmitter and receiver (transmitter on the cone axis) in the expected fashion.

The formula obtained by this method is

$$\sigma(\beta) = \frac{\lambda^2 \tan^4 \gamma}{16\pi} \frac{2(1 + \cos 2\gamma)}{(1 + \cos \beta)(\cos 2\gamma + \cos \beta)} \left[ \left( \frac{1 + \cos 2\gamma}{\cos 2\gamma + \cos \beta} \right)^2 + 2 \left( \frac{1 + \cos 2\gamma}{\cos 2\gamma + \cos \beta} \right) \left( \frac{1 - \cos \beta}{1 + \cos \beta} \right) \cos 2\phi + \left( \frac{1 - \cos \beta}{1 + \cos \beta} \right)^2 \right] \quad (5.2-9)$$

where  $\phi$  is the angle between the plane of polarization of the incident field, and the plane containing the axis of the cone and the receiver.

For back scattering,  $\beta = 0$ , (5.2-9) reduces to

$$\sigma(0) = \frac{\lambda^2 \tan^4 \gamma}{16\pi} \quad (5.2-10)$$

which is just the well known physical-optics result for back-scattering. It has previously been shown (Ref. 5) that the physical-optics answer agrees with the exact back-scattering answer both for large cone angles and for small cone angles.

The physical-optics bistatic cross-section of a semi-infinite cone given above is independent of  $\phi$ . Since the Luneberg-Kline solution is not independent of  $\phi$  it is clear that the two solutions do not agree exactly.

From (5.2-9) it can be seen that the maximum cross-section is obtained when  $\phi = 0$  and  $\phi = \pi$ , while the minimum cross-section is obtained for  $\phi = \pi/2$  and  $\phi = 3\pi/2$ . In Figure 13 the maximum and minimum cross-sections and the physical-optics approximation are plotted as a function of  $\beta$  for  $\gamma = 15^\circ$ . This graph shows that the physical-optics answer agrees very well with the Luneberg-Kline answer and that it lies approximately halfway between the maximum and minimum "Luneberg-Kline" curves.

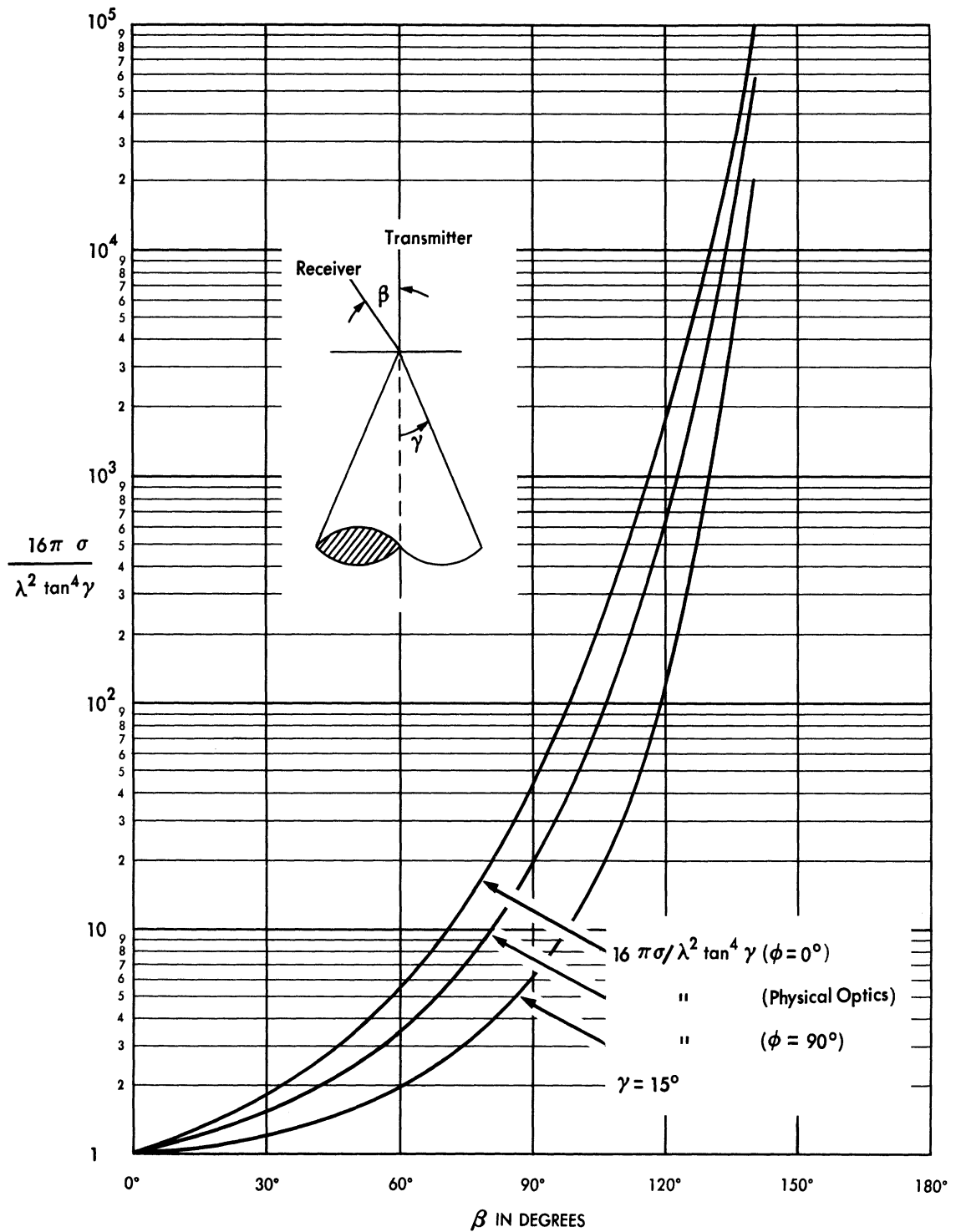


FIG. 13 BISTATIC CROSS-SECTION OF A SEMI-INFINITE CONE OF HALF-ANGLE  $15^\circ$

VI

BISTATIC CROSS-SECTIONS FOR ARBITRARY TRANSMITTER AND RECEIVER DIRECTIONS

6.1: The Elliptic Cylinder

Consider an elliptic cylinder with semi-major axis  $a$  and semi-minor axis  $b$  oriented with respect to the transmitter and the receiver as shown in Figure 14.

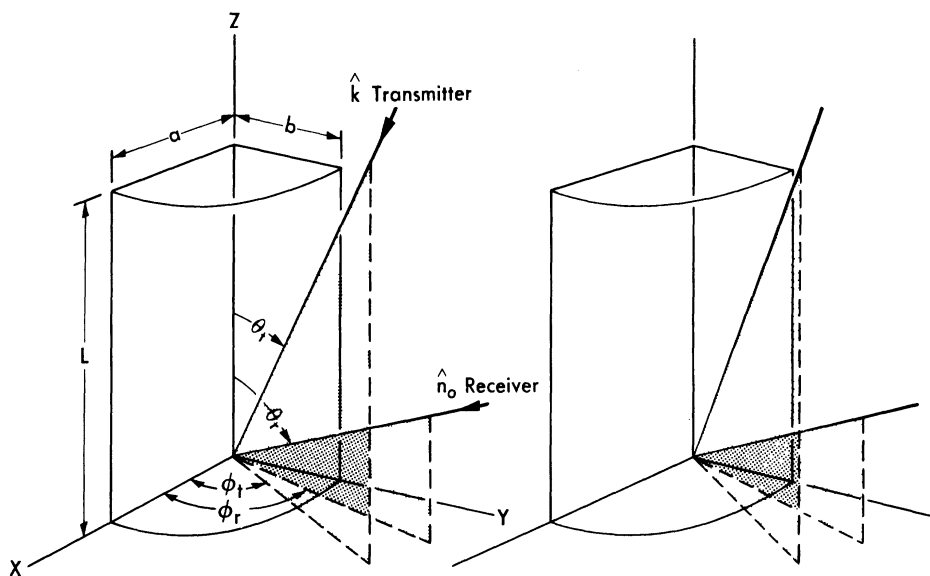


FIG. 14 GEOMETRY FOR THE ELLIPTIC CYLINDER

The Figure on the left is complete in itself. The other view is provided so that a three dimensional effect may be obtained by the use of a stereo viewer.

The angular positions of the transmitter and receiver are designated by

$\theta_t, \phi_t$  and  $\theta_r, \phi_r$  respectively.

By definition, the radar cross-section is given by

$$\sigma = 4\pi \left\{ |F_x|^2 + |F_y|^2 + |F_z|^2 \right\} \tag{6.1-1}$$



$$\text{where } \vec{F}(\theta_t, \theta_r, \phi_t, \phi_r) = \frac{-ik}{2\pi} (\hat{n}_o \cdot \hat{a}) \int_{\text{illuminated portion of the surface}} e^{ik\vec{r} \cdot (\hat{k} + \hat{n}_o)} \hat{n} dS$$

$$+ \frac{ik \hat{a}}{2\pi} \int_{\text{illuminated portion of the surface}} e^{ik\vec{r} \cdot (\hat{k} + \hat{n}_o)} (\hat{n}_o \cdot \hat{n}) dS,$$

and all the other parameters are as defined in Sec. 3.2. The problem of finding the cross-section is the problem of evaluating the integrals. This evaluation can be accomplished most simply in elliptic cylindrical coordinates ( $\xi, \eta, z$ ).\*

In this coordinate system the element of surface area,  $ds$ , is

$$ds = \sqrt{b^2 + c^2 \sin^2 \eta} d\eta dz$$

and the unit normal,  $\hat{n}$  is

---

\*These coordinates are related to Cartesian coordinates by the relations

$$x = c \cosh \xi \cos \eta$$

$$y = c \sinh \xi \sin \eta$$

$$z = z$$

where  $\xi = \xi_o = \text{constant}$  gives an elliptic cylinder with semi-axes  $a = c \cosh \xi_o$  and  $b = c \sinh \xi_o$  and  $c$  is related to the eccentricity and the semi-axes of the ellipse by

$$e = c/a = (1/a) \sqrt{a^2 - b^2}.$$

$$\hat{n} = \hat{i}_\xi = \hat{i}_x \left\{ \frac{b \cos \eta}{\sqrt{b^2 + c^2 \sin^2 \eta}} \right\} + \hat{i}_y \left\{ \frac{a \sin \eta}{\sqrt{b^2 + c^2 \sin^2 \eta}} \right\}.$$

Also,

$$\hat{k} = -\hat{i}_x \sin \theta_t \cos \phi_t - \hat{i}_y \sin \theta_t \sin \phi_t - \hat{i}_z \cos \theta_t$$

$$\hat{n}_o = -\hat{i}_x \sin \theta_r \cos \phi_r - \hat{i}_y \sin \theta_r \sin \phi_r - \hat{i}_z \cos \theta_r$$

$$\vec{r} = x\hat{i}_x + y\hat{i}_y + z\hat{i}_z,$$

so that the phase factor becomes

$$\begin{aligned} \vec{r} \cdot (\hat{n}_o + \hat{k}) = & x \left\{ \sin \theta_t \cos \phi_t + \sin \theta_r \cos \phi_r \right\} + y \left\{ \sin \theta_t \sin \phi_t \right. \\ & \left. + \sin \theta_r \sin \phi_r \right\} + z \left\{ \cos \theta_t + \cos \theta_r \right\}. \end{aligned}$$

By using the above relationships, the first integral appearing in (6.1-1) becomes

$$\int_s e^{-ik\vec{r} \cdot (\hat{k} + \hat{n}_o)} \hat{n} ds = \int_s \hat{i}_\xi e^{ik[Ax + By + Dz]} \sqrt{b^2 + c^2 \sin^2 \eta} d\eta dz$$

where  $A = \sin \theta_t \cos \phi_t + \sin \theta_r \cos \phi_r$

$B = \sin \theta_t \sin \phi_t + \sin \theta_r \sin \phi_r$

$D = \cos \theta_t + \cos \theta_r.$

Since  $x = c \cosh \xi_0 \cos \eta$ ,  $y = c \sinh \xi_0 \sin \eta$ ,  $z = z$ , this integral becomes

$$\int_s \hat{i}_\xi e^{ik [A c \cosh \xi_0 \cos \eta + B c \sinh \xi_0 \sin \eta + Dz]} \sqrt{b^2 + c^2 \sin^2 \eta} \, d\eta dz$$

Integrating with respect to  $z$  first,

$$\int_s e^{-ik\vec{r} \cdot (\hat{k} + \hat{n}_0)} \hat{n}_s ds = \frac{e^{ikDL} - 1}{ikD} \int_\eta \hat{i}_\xi e^{ik [A a \cos \eta + B b \sin \eta]} \sqrt{b^2 + c^2 \sin^2 \eta} \, d\eta.$$

Then using the method of stationary phase to integrate with respect to  $\eta$

$$\begin{aligned} & \int_\eta \hat{i}_\xi e^{ik [A a \cos \eta + B b \sin \eta]} \sqrt{b^2 + c^2 \sin^2 \eta} \, d\eta \\ &= \left(\frac{2\pi}{k}\right)^{1/2} \left| (Aa)^2 + (Bb)^2 \right|^{-1/4} \left[ \frac{\hat{i}_x A a b + \hat{i}_y B a b}{[(Aa)^2 + (Bb)^2]^{1/2}} \right] \exp \left\{ ik \left[ (Aa)^2 + (Bb)^2 \right]^{1/2} - i\frac{\pi}{4} \right\}. \end{aligned}$$

Therefore

$$\begin{aligned} & \frac{-ik}{2\pi} (\hat{n}_0 \cdot \hat{a}) \int \hat{i}_\xi e^{-ik\vec{r} \cdot (\hat{k} + \hat{n}_0)} \, ds \\ &= \left[ a_x \sin \theta_r \cos \phi_r + a_y \sin \theta_r \sin \phi_r + a_z \cos \theta_r \right] \left[ \frac{e^{ikDL} - 1}{2\pi D} \right] \lambda^{1/2} ab \\ & \cdot \frac{(\hat{i}_x A + \hat{i}_y B)}{[(Aa)^2 + (Bb)^2]^{3/4}} \exp \left\{ ik \left[ (Aa)^2 + (Bb)^2 \right]^{1/2} - i\pi/4 \right\}. \end{aligned} \tag{6.1-2}$$

In evaluating the second integral in (6.1-1), it should be noted that since the phase factor for this integral is the same as the phase factor of the integral evaluated above, the stationary-phase value does not change. Therefore

$$\int_s e^{-ik\vec{r} \cdot (\hat{n}_o + \hat{k})} ds \quad (6.1-3)$$

$$= -\sin\theta_r \left[ \frac{e^{ikDL} - 1}{ikD} \right] \lambda^{1/2} \frac{ab[A\cos\phi_r + B\sin\phi_r]}{[(Aa)^2 + (Bb)^2]^{3/4}} \exp\left\{ ik[(Aa)^2 + (Bb)^2]^{1/2} - i\frac{\pi}{4} \right\}.$$

Finally, from (6.1-1), (6.1-2), and (6.1-3)

$$\sigma(\theta_r, \theta_t, \phi_r, \phi_t) = \frac{a^2 b^2 \lambda \left| e^{ikDL} - 1 \right|^2}{\pi D^2 [(Aa)^2 + (Bb)^2]^{3/2}} \left\{ G_1^2 + G_2^2 + G_3^2 \right\} \quad (6.1-4)$$

where

$$G_1 = A(a_y \sin\theta_r \sin\phi_r + a_z \cos\theta_r) - B(a_x \sin\theta_r \sin\phi_r)$$

$$G_2 = a_z \sin\theta_r (A \cos\phi_r + B \sin\phi_r)$$

$$G_3 = B(a_x \sin\theta_r \cos\phi_r + a_z \cos\theta_r) - A(a_y \sin\theta_r \cos\phi_r)$$

$$A = \sin\theta_t \cos\phi_t + \sin\theta_r \cos\phi_r$$

$$B = \sin\theta_t \sin\phi_t + \sin\theta_r \sin\phi_r$$

$$D = \cos\theta_t + \cos\theta_r$$

$L$  = length of the elliptic cylinder

$a$  = semi-major axis

$b$  = semi-minor axis

$a_x, a_y, a_z$  = the x, y, and z components of the vector  $\hat{a}$

and  $\lambda = 2\pi/k$  = the wavelength.

For the special case of back-scattering in which  $\theta_t = \theta_r = \theta$  and  $\phi_t = \phi_r = \phi$  (6.1-4) becomes

$$\sigma(\theta, \phi) = \frac{a^2 b^2 \lambda \left| e^{ikDL} - 1 \right|^2 \sin^4 \theta}{\pi \cos^2 \theta \left[ (Aa)^2 + (Bb)^2 \right]^{3/2}} \quad (6.1-5)$$

Figure 15 is a plot of the  $\sigma$  of (6.1-4) versus  $\phi_r$  for the special case defined by  $\theta_r = \theta_t = \pi/2$  and  $\phi_t = 0$ . For this case (6.1-4) reduces to

$$\sigma(\phi_r) = \frac{4\pi b^2 L^2}{\lambda a} \frac{(1 + \cos \phi_r)^2}{\left[ (1 + \cos \phi_r)^2 + \left(\frac{b}{a}\right)^2 \sin^2 \phi_r \right]^{3/2}} \quad (6.1-6)$$

where  $a_x = 0$ .

## 6.2: The Prolate and Oblate Spheroids for Particular Choices of Transmitter and Receiver Directions

In Section 4.1 the bistatic cross-section of a prolate spheroid was determined for the case in which the transmitter is located on the axis of symmetry. In this section it will be shown that for each transmitter position (not necessarily on the symmetry axis) there is one particular

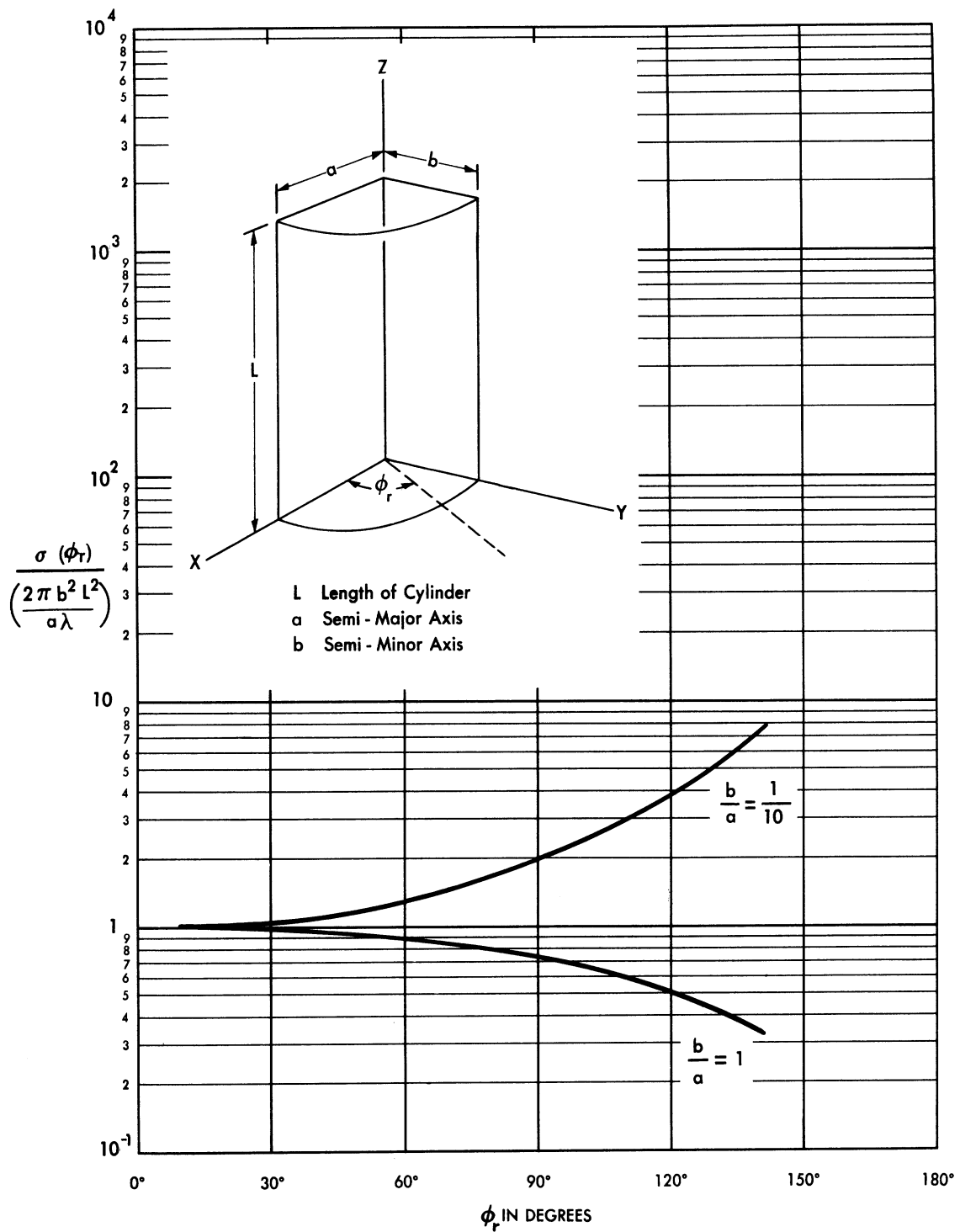


FIG. 15 BISTATIC CROSS-SECTION OF AN ELLIPTIC CYLINDER FOR THE CASE OF TRANSMITTER AND RECEIVER IN A PLANE PERPENDICULAR TO THE AXIS OF THE CYLINDER

receiver direction for which the current-distribution integral can be evaluated exactly, both for a prolate and an oblate spheroid.

According to the current-distribution method the bistatic radar cross-section is given by

$$\sigma = \frac{4\pi}{\lambda^2} |\vec{g}|^2 \quad (6.2-1)$$

where

$$\vec{g} = (\hat{n}'_o \cdot \vec{f}) \hat{a} - (\hat{n}'_o \cdot \hat{a}) \vec{f}$$

$$\vec{f} = \int_S \hat{n} e^{ik(\hat{n}'_o + \hat{k}_1) \cdot \vec{r}} dS$$

$S$  is the part of the surface seen by the transmitter,

$\hat{n}'_o$  is the direction to the receiver,

$\hat{k}_1$  is the direction to the transmitter,

$\hat{a}$  is the magnetic polarization of the incident radiation,

$\lambda = 2\pi/k$  is the wavelength, and

$\hat{n}$  is the normal to the surface.

If  $S^*$  is a second surface bounded by the shadow curve and  $V$  is the volume contained between  $S$  and  $S^*$  then

$$\begin{aligned} \vec{f} &= \int_S \hat{n} e^{ik(\hat{n}'_o + \hat{k}_1) \cdot \vec{r}} dS = \int_S (\hat{n} \cdot \vec{I}) e^{ik(\hat{n}'_o + \hat{k}_1) \cdot \vec{r}} dS \\ &= \int_V \text{div} \left\{ \vec{I} e^{ik(\hat{n}'_o + \hat{k}_1) \cdot \vec{r}} \right\} dV - \int_{S^*} \hat{n} e^{ik(\hat{n}'_o + \hat{k}_1) \cdot \vec{r}} dS \end{aligned}$$

$$= ik(\hat{n}'_0 + \hat{k}_1) \int_V e^{ik(\hat{n}'_0 + \hat{k}_1) \cdot \vec{r}} dV - \int_{S^*} \hat{n} e^{ik(\hat{n}'_0 + \hat{k}_1) \cdot \vec{r}} dS$$

where  $\hat{I}$  is the unit dyadic.

If  $\rho$  is chosen so that  $(\hat{n}'_0 + \hat{k}_1) \cdot \vec{r} = |\hat{n}'_0 + \hat{k}_1| \rho = 2\rho \cos \frac{\beta}{2}$   
 ( $\beta$  is the angle of separation between transmitter and receiver) then

$$\vec{f} = ik(\hat{n}'_0 + \hat{k}_1) \int e^{2ik\rho \cos(\beta/2)} A(\rho) d\rho - \int_{S^*} \hat{n} e^{ik(\hat{n}'_0 + \hat{k}_1) \cdot \vec{r}} dS \quad (6.2-2)$$

where  $A(\rho)$  is the area of the intersection of the volume  $V$  with the plane  $\rho = s$ . The plane  $\rho = s$  is a plane of constant phase or a phase plane. For a spheroid,  $S^*$  can always be chosen as the interior of an ellipse so that the second integral is easy to evaluate. If  $S^*$  lies in a phase plane,  $A(\rho)$  is a polynomial and the first integral is also easy to evaluate. This case is the particular case for which the cross-section integrals can be evaluated exactly.

The geometry used in this evaluation is shown in Figure 16. The axis of the spheroid,  $\hat{n}'_0$ , and  $\hat{k}_1$  all lie in the same plane. The angle between the axis and the normal to the phase planes is  $\beta_1$ . The angular separation between the transmitter, T, and the receiver, R, is  $\beta$ . For this geometry  $A(\rho)$  is given by

$$A(\rho) = \pi \frac{AB^2}{\rho_0^3} \left[ \rho_0^2 - \rho^2 \right] \quad (6.2-3)$$

where

$$\rho_0^2 \equiv A^2 \cos^2 \beta_1 + B^2 \sin^2 \beta_1.$$



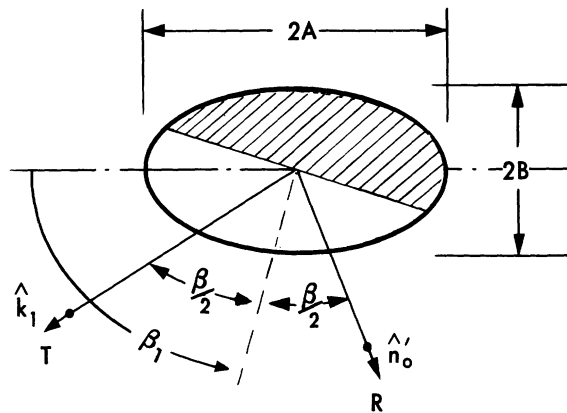


FIG. 16 GEOMETRY FOR PROLATE SPHEROID

The substitution of (6.2-3) into (6.2-2) gives

$$\vec{f} = -\frac{\pi AB^2}{\rho_0} \left\{ \frac{\hat{n}'_0 + \hat{k}_1}{\left[ \hat{n}'_0 + \hat{k}_1 \right]} \right\} \left[ \frac{1 - e^{2ik\rho_0 \cos(\beta/2)}}{2k^2 \rho_0^2 \cos^2(\beta/2)} + \frac{i e^{2ik\rho_0 \cos(\beta/2)}}{k \rho_0 \cos(\beta/2)} \right] \quad (6.2-4)$$

Then, substituting equation (6.2-4) into equation (6.2-1)

$$\sigma = \frac{\pi A^2 B^4}{\rho_0^4} \left[ 1 - 2 \frac{\sin(2X)}{2X} + \frac{\sin^2(X)}{X^2} \right] \quad (6.2-5)$$

where  $X = k \rho_0 \cos(\beta/2)$ .

Equation (6.2-5) applies only when the shadow curve lies in a phase plane. This condition is satisfied when

$$\tan(\beta/2) = \frac{A^2 - B^2}{\rho_0^2} \cdot \sin \beta_1 \cos \beta_1. \quad (6.2-6)$$

The maximum separation between transmitter and receiver which is obtainable is given by

$$\tan(\beta/2) = \frac{A^2 - B^2}{2AB} \quad \text{and} \quad \tan(\beta_1) = A/B.$$

Figure 17 shows the cross-section of the prolate spheroid ( $kB = 2.5$  and  $kA = 25$ ) as a function of the receiver angle with the corresponding transmitter angle, determined from Equation (6.2-6), indicated at regular intervals. The range in the receiver angle shown in the figure is from  $0^\circ$  up to  $162.9^\circ$  which is the receiver angle corresponding to the maximum separation obtainable for  $A/B = 10$ .

The method used in this section could also be applied to other quadric surfaces. For example, special cases could be integrated exactly for an ellipsoid having three non-equal axes.

### 6.3: Determination of $\sigma$ by Numerical Integration Techniques

The determination of  $\sigma$  by the current-distribution method involves the evaluation of an integral of the form

$$\int_{\text{illuminated portion of the body}} \hat{n} \exp \left\{ i\vec{k}r \cdot (\hat{n}_0 + \hat{k}) \right\} dS. \quad (6.3-1)$$

illuminated portion  
of the body

This integral is, in general, difficult to evaluate in a form which lends itself readily to the determination of numerical values of  $\sigma$ . However, it can be approximated for use in numerical computations as follows:

Planes of constant phase (phase planes) are planes which are defined by an equation of the form

$$(\hat{n}_0 + \hat{k}) \cdot \vec{r} = c$$

where  $c$  is a constant for each particular plane. Let  $r_0$  represent the radius vector from the origin to the point at which these planes first

UMM-115

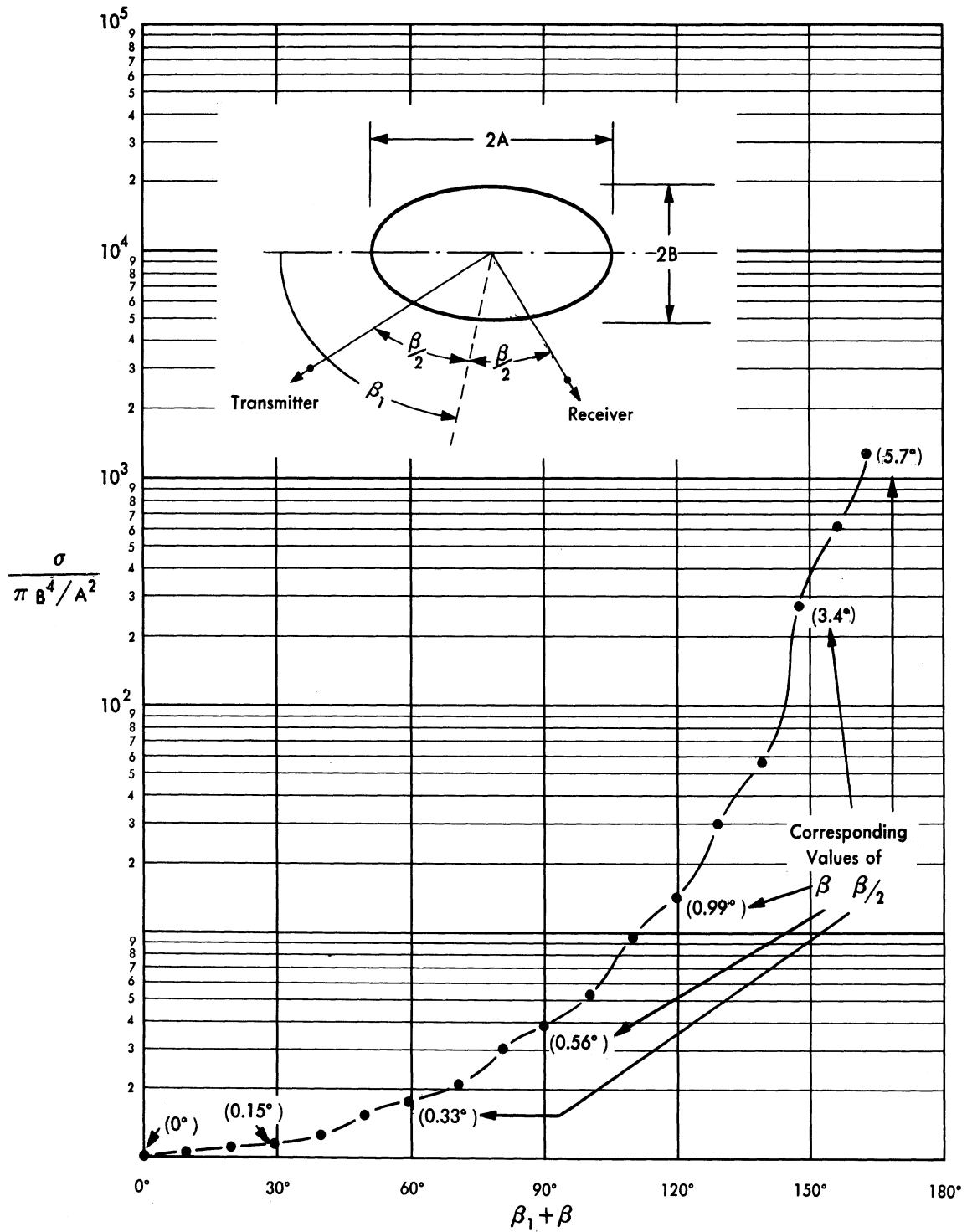


FIG. 17 BISTATIC CROSS - SECTION OF A PROLATE SPHEROID

strike the body. For a smooth body this point corresponds to a stationary phase point while for a conical tip this point, in certain cases, is the tip of the body. Let  $\rho$  represent the distance of each point on the body from the "first phase plane".

Let  $\hat{i}_x$ ,  $\hat{i}_y$ , and  $\hat{i}_z$  represent three orthogonal vectors forming the base for a Cartesian coordinate system and let  $x$ ,  $y$ , and  $z$  be the corresponding coordinates. Let  $A(\rho)_x$  be the area of the illuminated portion of the body up to the phase plane which is located at a distance of  $\rho$  from the first phase plane projected in the  $\hat{i}_x$  direction. In projecting, care must be taken to count the contribution of those regions of the body for which  $n_x$  is negative as negative area.  $A(\rho)_y$  and  $A(\rho)_z$  are defined analogously. In terms of these functions the integral (6.3-1) can be written as

$$\int_R e^{ik(\hat{n}_o + \hat{k}) \cdot \vec{r}} \hat{n} dS = \hat{i}_x \int_{\rho_0}^{\rho = \rho_{end}} \exp \left\{ ik \left| \hat{n}_o + \hat{k} \right| \rho \right\} dA(\rho)_x \quad (6.3-2)$$

$$+ \hat{i}_y \int_{\rho_0}^{\rho = \rho_{end}} \exp \left\{ ik \left| \hat{n}_o + \hat{k} \right| \rho \right\} dA(\rho)_y$$

$$+ \hat{i}_z \int_{\rho_0}^{\rho = \rho_{end}} \exp \left\{ ik \left| \hat{n}_o + \hat{k} \right| \rho \right\} dA(\rho)_z .$$

If the area functions  $A(\rho)_x$ ,  $A(\rho)_y$ , and  $A(\rho)_z$  cannot be expressed analytically or if the analytic functions lead to integrals which are difficult to evaluate, then polynomial approximations to these area functions can be used in (6.3-2). The best results will be obtained when these polynomial approximations have the same degree of "smoothness" as the area functions; that is, if the actual area functions have a continuous first derivative for all  $\rho$  in the interval of integration then the polynomial representation should have a continuous first derivative in the interval of integration.

This method can be modified so that it is readily applicable to those cases for which the shadow curve is a plane curve. Such is the case, for example, for all quadric surfaces. For surfaces such as the ogive the "shadow" curve is plane only when the transmitter is nose-on or broad-side. This modification is accomplished as follows: transform the surface integral (6.3-1) into the sum of a volume integral over the volume enclosed by the surface and the shadow plane ( V ) and of a surface integral over that region of the shadow plane which is bounded by the shadow curves ( S ). This procedure yields

$$\begin{aligned}
 \int_R e^{ik(\hat{n}_o + \hat{k}) \cdot \vec{r}} \hat{n} dS &= \hat{i}_x \int_V \operatorname{div} \left\{ \hat{i}_x e^{ik(\hat{n}_o + \hat{k}) \cdot \vec{r}} \right\} dV \\
 &+ \hat{i}_y \int_V \operatorname{div} \left\{ \hat{i}_y e^{ik(\hat{n}_o + \hat{k}) \cdot \vec{r}} \right\} dV \\
 &+ \hat{i}_z \int_V \operatorname{div} \left\{ \hat{i}_z e^{ik(\hat{n}_o + \hat{k}) \cdot \vec{r}} \right\} dV \\
 &- \int_S \hat{n} e^{ik(\hat{n}_o + \hat{k}) \cdot \vec{r}} dS \quad (6.3-3)
 \end{aligned}$$

If  $A(\rho)$  is the cross-sectional area of the body cut by the phase plane which is a distance  $\rho$  away from the reference plane (the first phase plane which strikes the body), then (6.3-3) can be written in the form,

$$\int_R e^{ik(\hat{n}_o + \hat{k}) \cdot \vec{r}} \hat{n} dS = ik(\hat{n}_o + \hat{k}) \int_{\rho=0}^{\rho=\rho_{\text{end}}} e^{ik|\hat{n}_o + \hat{k}| \rho} A(\rho) d\rho - \hat{n}' \int_S e^{ik(\hat{n}_o + \hat{k}) \cdot \vec{r}} dS$$

where  $\hat{n}'$  is the outward normal to the "shadow" plane.

The surface integral on the right is readily evaluated for a wide variety of shadow curve shapes so that the main concern is the evaluation of the volume integral. The advantage of this particular representation over the previous more general one is that there is only one integral to approximate instead of three and that negative areas do not appear.

The area function  $A(\rho)$  can be evaluated analytically or graphically at various points and polynomial approximations can be constructed which can be used for  $A(\rho)$  in the integral.

## VII

## CONCLUSION

Approximate formulas have been derived for the bistatic radar cross-section of simple geometric shapes. These formulas, together with the formulas for the monostatic cross-section of these shapes, are listed in Table 1 on the following page. This table is the first catalog of bistatic cross-section formulas, one which can readily be extended to include other configurations upon application of the methods presented in this paper.\* In addition, each of the bistatic formulas has been applied to a specific problem and the answer to these problems has been presented in graphical form. The reciprocity relationships make it possible to apply the bistatic formulas of Table 1 to the reciprocal case in which the positions of the transmitter and receiver are interchanged.

Evidence is presented in this paper in favor of using the current-distribution method as a method of approximation when the wavelength is small with respect to the characteristic dimension of the body. The results in Section 4 lead to the conclusion that for small wavelengths application of the method of stationary phase to the problem of evaluating  $\sigma$  is sufficient for most practical purposes. Figures 5, 6, and 9 show that if the method of stationary phase is applicable, then the results obtained from this method are as good as those obtained from a combination of exact integration and analog computer integration for most values of  $\beta$ . The results obtained for the paraboloid and the semi-infinite cone give strong support to the belief that the methods used in this paper, including an Abelian limit process, suffice for determining the cross-section of semi-infinite bodies which are entirely "illuminated".

---

\*Appendix 5 contains two tables of cross-section formulas for a few bodies not considered in this report; these formulas are readily obtainable upon application of the methods discussed in this paper.

TABLE 1  
APPROXIMATE MONOSTATIC AND BISTATIC CROSS-SECTION FORMULAS<sup>1</sup>

Type of Body	Orientation of Body with Respect to Transmitter and Receiver	Monostatic, Back-Scattering Cross-Section <sup>2</sup>	Bistatic, Scattering Cross-Section $\sigma_{\hat{a}=\hat{y}}(\beta)$	Code to Symbols	
Prolate Spheroid	Direction of the Polarization of the incident wave is defined by $\hat{a} = \hat{y}$ . Direction of Propagation is parallel to the axis of symmetry of the body. The Receiver is located in the yz-plane ( $y < 0$ ). (See Figure 3)	$\pi B^4/A^2$	$\frac{4\pi B^4/A^2}{\left[ (1 + \cos \beta) + \frac{B^2}{A^2}(1 - \cos \beta) \right]^2}$ ( $0 \leq \beta < \pi$ )	A = semi-major axis B = semi-minor axis	
Sphere		$\pi R^2$	$\pi R^2$ ( $0 \leq \beta < \pi$ )	R = radius of sphere	
Ogive		$\frac{\lambda^2 \tan^4 \alpha}{16\pi}$	$\frac{\lambda^2 \tan^4 \alpha}{16\pi} \frac{(1 - \tan^2 \alpha \tan^2(\beta/2))^{-3}}{\cos^8(\beta/2)}$ ( $0 \leq \beta < \pi - 2\alpha$ ) $\frac{\pi L^2 [\sin(\beta/2) - \cos \alpha]}{4 \sin^2 \alpha \sin(\beta/2)}$ ( $\pi - 2\alpha \leq \beta < \pi$ )	$\alpha = 1/2$ nose-angle L = length of ogive	
Finite Cone		$\pi r_o^2 \sin^2 \gamma \tan^2 \gamma$	$\frac{4\pi r_o^2 \sin^4 \gamma}{(b^2 - c^2)^2} \left[ c^2 [J_0(u)]^2 + b^2 [J_1(u)]^2 \right]$ where $u = \frac{2\pi r_o b}{\lambda}$ . ( $0 \leq \beta < \pi - 2\gamma$ )	$\gamma = 1/2$ nose-angle $r_o$ = slant length of cone $b = \sin \gamma \sin \beta$ $c = \cos \gamma (1 + \cos \beta)$ $J_0$ and $J_1$ = Bessel functions of order zero and one respectively.	
The Paraboloid		$4\pi p^2$	$\frac{16\pi p^2}{(1 + \cos \beta)^2}$ <sup>3</sup>	Surface defined by the equation $z = -4pr^2$ (cylindrical coord.)	
Semi-Infinite Cone		$\frac{\lambda^2 \tan^4 \gamma}{16\pi}$	$\frac{\lambda^2 \tan^4 \gamma}{16\pi} \cdot \frac{2(1 + \cos 2\gamma)^3}{(1 + \cos \beta)(\cos \beta + \cos 2\gamma)^3}$ ( $0 \leq \beta < \pi - 2\gamma$ )	$\gamma = 1/2$ nose-angle	
The Elliptic Cylinder		(See Figure 14)	$\frac{a^2 b^2 \lambda^2}{\pi \cos^2 \theta} \left  \frac{e^{ikDL} - 1}{(Aa)^2 + (Bb)^2} \right ^2 \frac{\sin^4 \theta}{2}$	(See Equation 6.1-4)	a = semi-major axis b = semi-minor axis L = length of cylinder A = $2 \sin \theta \cos \theta$ B = $2 \sin \theta \sin \theta$ D = $2 \cos \theta$ k = $2\pi/\lambda$

<sup>1</sup>These formulas hold when the wavelength is small with respect to the characteristic dimension of the body.

<sup>2</sup>For all entries in this column except that for the Elliptic Cylinder the back-scattering answer is given by  $\beta = 0$ . In the case of the Elliptic Cylinder a more general monostatic result is presented.

<sup>3</sup>This formula is exact (Sec. 5.1).



APPENDIX I

PROOF OF THE DOUBLE STATIONARY-PHASE THEOREM

Theorem: Let  $I = \int_c^d \int_a^b f(x, y) e^{iKg(x, y)} dx dy.$

If 1)  $f(x, y) = X(x)Y(y)$  is analytic in the region  $R = \{x, y \mid a \leq x \leq b, c \leq y \leq d\};$

2)  $g(x, y)$  is analytic in  $R;$

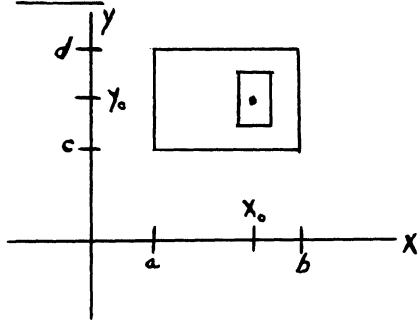
3) there exists one and only point  $(x_0, y_0)$ , in the interior of  $R$ , such that  $p_0 = q_0 = 0$  and  $r_0 t_0 - s_0^2 \neq 0$ , where  $p, q, r, s, t$  are the usual partial derivatives of  $g^*$ , and

4)  $X(\xi)/g_\xi(\xi, \eta)$  and  $Y(\eta)/g_\eta(\xi, \eta)$  are of bounded variation for  $(\xi, \eta)$  in  $R$  but not in  $R' = \{x, y \mid x_0 - \delta \leq x \leq x_0 + \delta, y_0 - \epsilon \leq y \leq y_0 + \epsilon\},$

then

$$I = \frac{\pm 2i\pi e^{iKg(x_0, y_0)} f(x_0, y_0)}{K [r_0 t_0 - s_0^2]^{1/2}} + O(1/K^{3/2}) \text{ as } K \rightarrow \infty .$$

Proof: Let  $I$  be written as



$$I = \int_c^d \int_a^{x_0 - \delta} + \int_c^{y_0 - \epsilon} \int_{x_0 - \delta}^{x_0 + \delta} + \int_{y_0 - \epsilon}^{y_0 + \epsilon} \int_{x_0 - \delta}^{x_0 + \delta} + \int_{y_0 + \epsilon}^d \int_{x_0 - \delta}^{x_0 + \delta} + \int_c^d \int_{x_0 + \delta}^b .$$

\*That is  $p = g_x, q = g_y, r = g_{xx}, s = g_{xy},$  and  $t = g_{yy}.$

In the regions indicated by the limits of integration of the first two and last two integrals,  $g$  is a monotone function in  $x$  and in  $y$  (since  $g_x$  and  $g_y$  do not vanish in  $R-R'$ ). Thus by a double application\* of Riemann's Lemma\*\* it can be argued that each of the first two and last two integrals is of the order  $1/K^2$  as  $K \rightarrow \infty$ . The middle integral (which will be called  $I_{\delta\epsilon}$ ) is:

$$I_{\delta\epsilon} = \iint_{R'} f(x, y) e^{iKg(x, y)} dx dy. \tag{A.1-1}$$

Replace  $g$  by

$$g \approx g_0 + \frac{1}{2} \left[ r_0(x-x_0)^2 + 2s_0(x-x_0)(y-y_0) + t_0(y-y_0)^2 \right]$$

and make the transformation

$$x - x_0 = u \cos\theta - v \sin\theta$$

$$y - y_0 = u \sin\theta + v \cos\theta$$

where  $\theta = \frac{1}{2} \arctan \frac{2s_0}{r_0-t_0}$ , [or  $\theta = 45^\circ$  if  $r_0 = t_0$ ].

Then

$$g \approx g_0 + [Au^2 + Bv^2],$$

where

$$A = \frac{r_0 + t_0 + \sqrt{(r_0 - t_0)^2 + 4s_0^2}}{4} \text{ and } B = \frac{r_0 + t_0 - \sqrt{(r_0 - t_0)^2 + 4s_0^2}}{4}.$$

\*The hypotheses are sufficiently strong to allow iteration of the double integrals.

\*\*Riemann's Lemma, (Ref. 20, p. 431) For any function  $f(x)$  of bounded variation

$$\int_a^b f(x) \cos Ax dx = O(1/A), \int_a^b f(x) \sin Ax dx = O(1/A).$$

The expression (A.1-1) can then be replaced by

$$I_{\delta\epsilon} = e^{iKg_0} \int_{-\tau}^{\tau} \int_{-\sigma}^{\sigma} F(u, v) e^{iK[Au^2 + Bv^2]} du dv$$

where the region  $-\tau \leq v \leq \tau$ ,  $-\sigma \leq u \leq \sigma$  is contained in the region  $R'$ .

Expand  $F(u, v)$  in a Taylor series about the point  $(x_0, y_0)$  and assume that its circle of convergence contains  $R'$ . Then the Taylor series is uniformly convergent in  $R'$  and \*

$$I_{\delta\epsilon} = e^{iKg_0} \sum_{n=0}^{\infty} \sum_{m=0}^n \frac{1}{n!} F_0^{[(n-m)u, mv]} \binom{n}{m} \iint_{R'} u^{n-m} v^m e^{iK[Au^2 + Bv^2]} du dv.$$

For  $n-m$  and/or  $m$  odd  $\iint_{R'} = 0$ . Integrating the remaining even powers by parts and letting  $U = \int_{-\sigma}^{\sigma} e^{iKAu^2} du$  and  $V = \int_{-\tau}^{\tau} e^{iKBv^2} dv$  yields

$$I_{\delta\epsilon} = e^{iKg_0} \left\{ UV \left[ \sum_{n=0}^{\infty} \sum_{m=0}^n \frac{(-1)^n}{n!} \binom{n}{m} \frac{F_0^{[2(n-m)u, 2mv]}}{(2iK)^n A^{n-m} B^m} \right] \right. \\ \left. + \frac{V\sigma e^{iKA\sigma^2}}{iKA} \left[ \sum_{m=1}^{\infty} \frac{(-1)^{m-1} \cdot 1 \cdot 3 \cdot 5 \cdots (2m-1)}{(2iKB)^{m-1}} \sum_{n=1}^{\infty} \frac{\binom{2n+2m-2}{2m-2}}{(2n+2m-2)!} \frac{(-1)^{n-1} F_0^{(2nu, 2mv)} \cdot 1 \cdot 3 \cdot 5 \cdots (2n-1)}{(2iKA)^{n-1}} \right] \right. \\ \left. + \frac{AV\sigma^3 e^{iKA\sigma^2}}{(2iKA)^3 (iKB)} \left[ \sum_{m=3}^{\infty} \frac{(-1)^{m-1} \cdot 1 \cdot 5 \cdots (2m-1)}{(2iKB)^{m-1}} \sum_{n=3}^{\infty} \frac{\binom{2n+2m-2}{2m-2}}{(2n+2m-2)!} \frac{(-1)^{n-1} F_0^{(2nu, 2mv)} \cdot 1 \cdot 5 \cdots (2n-1)}{(2iKA)^{n-1}} \right] \right\}$$

\*  $F_0^{(nu, mv)}$  indicates the mixed partial derivative of  $F$  with respect to  $u$  and  $v$ ,  $n$  times with respect to  $u$  and  $m$  times with respect to  $v$ , evaluated at  $(x_0, y_0)$ .

$$\begin{aligned}
 & + \dots + \frac{U\tau e^{iKB\tau^2}}{iKB} \left[ \sum_{m=1}^{\infty} \frac{(-1)^{m-1} \cdot 1 \cdot 3 \cdot 5 \cdots (2m-1)}{(2iKA)^{m-1}} \sum_{n=1}^{\infty} \frac{\binom{2n+2m-2}{2m-2}}{(2n+2m-2)!} \frac{(-1)^{n-1} F_0(2nu, 2mv) \cdot 1 \cdot 3 \cdot 5 \cdots (2n-1)}{(2iKB)^{n-1}} \right] \\
 & + \frac{BU\tau^3 e^{iKB\tau^2}}{(2iKB)^3 (iKA)} \left[ \sum_{m=3}^{\infty} \frac{(-1)^{m-1} \cdot 1 \cdot 5 \cdots (2m-1)}{(2iKA)^{m-1}} \sum_{n=3}^{\infty} \frac{\binom{2n+2m-2}{2m-2}}{(2n+2m-2)!} \frac{(-1)^{n-1} F_0(2nu, 2mv) \cdot 1 \cdot 5 \cdots (2n-1)}{(2iKB)^{n-1}} \right]
 \end{aligned}$$

+ ... + [similar terms in products of powers of  $\sigma$  and  $\tau$  (with no U and V factors) which are of order  $1/K^j$ ,  $j \geq 2$ ]

The result of integrating the uniformly convergent Taylor series [each term of which is multiplied by  $e^{iK(Au^2 + Bv^2)}$ ] is an absolutely convergent series in  $R'$  and hence may be rearranged as above.

Thus

$$I_{\delta\epsilon} = e^{iKg_0} \left[ UVF_0 + UV \cdot O(K^{-1}) + V \cdot O(K^{-1}) + U \cdot O(K^{-1}) + O(K^{-2}) \right] \tag{A.1-2}$$

Since

$$U = \int_{-\sigma}^{\sigma} e^{iKAu^2} du \approx \frac{(1 \pm i)\pi^{1/2}}{(KA)^{1/2}} \quad \text{and} \quad V = \int_{-\tau}^{\tau} e^{iKBv^2} dv \approx \frac{(1 \pm i)\pi^{1/2}}{(KB)^{1/2}} \quad *$$

U and V are both of the order  $K^{-1/2}$ ; (A.1-2) may be rewritten as

$$I = e^{iKg_0} \left[ UVF_0 + O(K^{-3/2}) \right] \quad \text{or}$$

$$I = I_{\delta\epsilon} + O(K^{-3/2}) .$$

\*Ref. 20, p. 473, Prob. 15; these are Fresnel integrals.

Therefore, using the above expressions for U and V, as  $K \rightarrow \infty$

$$I = \frac{\pm 2\pi i e^{iKg(x_0, y_0)} f(x_0, y_0)}{K [r_0 t_0 - s_0^2]^{1/2}} + O(K^{-3/2}).$$

## APPENDIX 2

DETERMINATION OF  $\sigma_{\hat{a}=1}^{\hat{a}}(\beta)$  BY THE D.S.P. THEOREM  
FOR THE PROLATE SPHEROID, THE SPHERE, AND THE OGIVE

The Prolate Spheroid by the D.S.P. Theorem

$$I_z = B^2 \int_0^1 \int_0^{2\pi} \eta e^{-ik [B \sin\beta \sin\theta \sqrt{1-\eta^2} - A(1+\cos\beta)\eta]} d\theta d\eta$$

$$f(\theta, \eta) = B^2 \eta$$

$$g(\theta, \eta) = -B \sin\beta \sin\theta \sqrt{1-\eta^2} + A(1+\cos\beta)\eta$$

$$(\theta_0, \eta_0) = \left( \frac{3\pi}{2}, \frac{A(1+\cos\beta)}{[B^2 \sin^2\beta + A^2(1+\cos\beta)^2]^{1/2}} \right)$$

$$\left\{ \begin{array}{l} r = \frac{\partial^2 g}{\partial \theta^2} = B \sin\beta \sin\theta \sqrt{1-\eta^2} \\ r_0 = \frac{-B^2 \sin^2\beta}{\sqrt{B^2 \sin^2\beta + A^2(1+\cos\beta)^2}} \end{array} \right.$$

$$\left\{ \begin{array}{l} s = \frac{\partial^2 g}{\partial \eta \partial \theta} = B \sin\beta \cos\theta (1-\eta^2)^{-1/2} \eta \\ s_0 = 0 \end{array} \right.$$

$$\left\{ \begin{array}{l} t = \frac{\partial^2 g}{\partial \eta^2} = B \sin\beta \sin\theta [\eta^2(1-\eta^2)^{-3/2} + (1-\eta^2)^{-1/2}] = B \sin\beta \sin\theta (1-\eta^2)^{-3/2} \\ t_0 = \frac{-[B^2 \sin^2\beta + A^2(1+\cos\beta)^2]^{3/2}}{B^2 \sin^2\beta} \end{array} \right.$$

$$\left| I_z \right|^2 = \frac{4\pi^2 \frac{A^2 B^4 (1 + \cos \beta)^2}{B^2 \sin^2 \beta + A^2 (1 + \cos \beta)^2}}{k^2 [B^2 \sin^2 \beta + A^2 (1 + \cos \beta)^2]} = \frac{4\pi^2 A^2 B^4 (1 + \cos \beta)^2}{[B^2 \sin^2 \beta + A^2 (1 + \cos \beta)^2]^2 k^2}$$

$$\sigma = \left| I_z \right|^2 \cdot \frac{k^2}{\pi} = \frac{4\pi B^4}{A^2 \left[ \frac{B^2}{A^2} (1 - \cos \beta) + (1 + \cos \beta) \right]^2}$$

#### The Sphere by the D.S.P. Theorem

The solution of the sphere problem is the same as that for the prolate spheroid problem except for the meaning of parameters. If both A and B in the prolate spheroid derivation are replaced by  $R_0$ , the derivation for the sphere is obtained. The cross-section of the sphere turns out to be

$$\sigma = \pi R_0^2.$$

#### The Ogive by the D.S.P. Theorem

$$I_z = \int_0^{p-h} \int_0^{2\pi} w e^{ik \left[ (1+\cos\beta)\sqrt{p^2-(w+h)^2} - w \sin\beta \sin\phi \right]} d\phi dw.$$

Apply the Theorem of D.S.P. using

$$f(w, \phi) = w; \quad g(w, \phi) = (1 + \cos \beta) \sqrt{p^2 - (w+h)^2} - w \sin \beta \sin \phi;$$

$$\frac{\partial g}{\partial \phi} = -w \sin \beta \cos \phi = 0 \text{ if } \phi = \frac{\pi}{2} \text{ or } \frac{3\pi}{2};$$

$$\frac{\partial g}{\partial w} = -(1 + \cos \beta) [p^2 - (w + h)^2]^{-1/2} (w + h) - \sin \beta \sin \phi,$$

$$(1 + \cos \beta) [p^2 - (w + h)^2]^{-1/2} (w + h) = \sin \beta \text{ if } \phi = \frac{3\pi}{2};$$

solving for  $w$ , yields  $w = p \sin \frac{\beta}{2} - h$ .

Since  $w \geq 0$ , and since  $\frac{h}{p} = \cos \alpha$ ,

$\beta$  is restricted to angles greater than or equal to  $\pi - 2\alpha$ .

Hence, the stationary-phase point is

$$(w_0, \phi_0) = \left( p \sin \frac{\beta}{2} - h, \frac{3\pi}{2} \right) \text{ where } \beta \geq \pi - 2\alpha.$$

Differentiating  $\frac{\partial g}{\partial \phi}$  and  $\frac{\partial g}{\partial w}$  with respect to  $\phi$  and  $w$  to find

$$r = \frac{\partial^2 g}{\partial w^2}, \quad s = \frac{\partial^2 g}{\partial w \partial \phi}, \quad t = \frac{\partial^2 g}{\partial \phi^2} \quad \text{yields}$$

$$r = -(1 + \cos \beta) \left\{ [p^2 - (w + h)^2]^{-1/2} + (w + h)^2 [p^2 - (w + h)^2]^{-3/2} \right\},$$

$$s = -\sin \beta \cos \phi,$$

$$t = w \sin \beta \sin \phi,$$



and

$$r_o = -\frac{2}{p \cos \frac{\beta}{2}},$$

$$s_o = 0,$$

$$t_o = -(p \sin \frac{\beta}{2} - h) \sin \beta, \beta \neq \pi.$$

Thus

$$|I_z|^2 = \frac{p\pi^2 (p \sin \frac{\beta}{2} - h)}{k^2 \sin \frac{\beta}{2}}$$

and

$$\sigma = |I_z|^2 \frac{k^2}{\pi} = \frac{p\pi (p \sin \frac{\beta}{2} - h)}{\sin \frac{\beta}{2}}, \text{ for } \pi > \beta \geq \pi - 2\alpha.$$

## APPENDIX 3

THE HANSEN AND SCHIFF TREATMENT OF  
BACK-SCATTERING FROM A SPINDLE

Hansen and Schiff in Reference 17 discuss back-scattering from a spindle. The integral expression which they obtain for the cross-section leads to a result which implies that the contributions from the tip and the shadow edge are of the same order of magnitude. They then consider the way in which the contribution from the shadow edge has to be altered to take account of the finite width of the transition region from light to shadow (the penumbra region).

Their discussion of the penumbra region is as follows:\*

"The width  $\ell$  of the penumbra region is expected to depend on the wavelength  $\lambda$  and on the radius of curvature  $R$  of the intersection of the body surface and a plane that is parallel to the direction of illumination and perpendicular to the shadow edge. We first give a qualitative physical argument which indicates that

$$\ell \sim (\lambda R^2)^{1/3}, \quad (7)$$

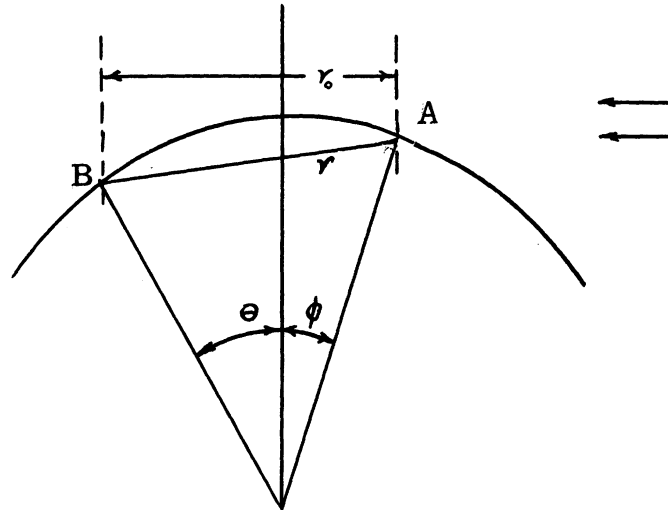
and then make use of a quantitative treatment (due to V. Fock) to show that the shadow edge contribution to  $g$  is of smaller order than the point contribution.

"The shadow may be thought of as being due to an interference between the incident plane wave and the secondary waves produced by the current elements induced in the front (illuminated) part of the scattering object. For short wavelengths, this interference is complete except near the edge of the geometrical shadow. We can thus obtain an order of magnitude estimate for  $\ell$  by finding the distance over which this interference is incomplete. In doing this we need consider only current

---

\*Note: The  $g$  used by Hansen and Schiff corresponds to the  $I_z(\beta = 0)$  used in this paper.

elements close to the shadow edge, since the effect of more distant elements is diminished by the inverse square law.



"In the diagram, the current element at A produces an effect at B with the path length  $r$ , which interferes with the plane wave that travels the path length  $r_0$ . For given  $\theta$ , the most effective elements will be those for which  $\phi$  is of order  $\theta$ , because of the inverse square law. We therefore determine the value of  $\theta$  (and  $\phi$ , which is of the same order of magnitude) such that the path difference  $r - r_0$  is of order  $\lambda$ . This determines the region of incomplete interference, and hence the penumbra.

"We see that

$$r = 2R \sin\left(\frac{\theta + \phi}{2}\right), \quad r_0 = R(\sin \theta + \sin \phi),$$

so that for small  $\theta$  and  $\phi$  :

$$r - r_0 \approx R \left[ \frac{\theta^3 + \phi^3}{6} - \frac{(\theta + \phi)^3}{24} \right].$$

Since  $\theta$  and  $\phi$  are of the same order, we see that

$$l \sim R\theta \quad \text{where} \quad R\theta^3 \sim \lambda,$$

from which it follows that  $l$  is given by equation (7).

"A quantitative treatment that leads to the same expression for  $\ell$ , and also gives the current density as a function of the distance from the geometrical shadow edge, has been given by V. Fock (Journal of Physics of the USSR, 10, 130 (1946)). He shows that the induced current in the shadow falls off approximately exponentially with the distance, the characteristic length being  $\ell$ ".

Hansen and Schiff then go on to say that this result suggests that the integral in question be supplemented by the inclusion of a contribution beyond the geometrical shadow edge. The net result being that if the wavelength is small with respect to the linear dimensions of the body then the point makes the dominant contribution to the cross-section.

It is of interest to compare the Hansen and Schiff results obtained for the spindle, the answers obtained for the ogive (Sec. 4.3), and the "exact" answer for the semi-infinite cone.

The results obtained by Hansen and Schiff are

$$\sigma_{\text{spindle}}(0) = \frac{\lambda^2 \tan^4 \theta_0}{16\pi}, \quad (\text{ignoring the contribution of the penumbra})$$

$$= \frac{\lambda^2 \tan^4 \theta_0}{16\pi} \left| e^{ikx_0} + \frac{1}{ik\ell} \right|^2, \quad (\text{using the contribution of the penumbra})$$

where  $\theta_0 = 1/2$  the nose-angle of the spindle,  $x_0 = 1/2$  the length of the spindle, and  $\ell \sim (\lambda R^2)^{1/3}$  where  $R$  = the radius of curvature of the intersection of the body surface and a plane that is parallel to the direction of illumination and perpendicular to the shadow edge.

It is readily obvious that with the "shadow" contribution neglected in each case, the ogive, the spindle, and the semi-infinite cone back-scattering cross-section formulas are identical.

## APPENDIX 4

## THE LUNEBERG-KLINE METHOD

Professor M. Kline (Ref. 18) has obtained an asymptotic expansion for solutions to Maxwell's equations which is valid for small wavelengths. The coefficients of this expansion are obtained recursively as the solutions of ordinary differential equations. As pointed out by Kline the equations for the coefficients can be obtained formally by assuming the existence of the asymptotic expansion. This formal development is as follows: Let the electric field be given by  $\vec{E} \exp(ik[\psi - ct])$  where  $\psi(x, y, z)$  is the real solution of the eikonal equation  $(\nabla \psi)^2 = 1$ , which, for large negative values of  $\psi$ , represents the phase of the incident plane wave. The requirements that the electric field satisfy the wave equation and have zero divergence then take the form

$$\nabla^2 \vec{E} + 2ik \frac{d\vec{E}}{ds} + ik \vec{E} \operatorname{div} \hat{s} = 0 \quad (\text{A.4-1})$$

$$\operatorname{div} \vec{E} + ik \hat{s} \cdot \vec{E} = 0 \quad (\text{A.4-2})$$

where  $\hat{s} \equiv \nabla \psi$  and  $\frac{d}{ds}$  is the directional derivative along the normal to the surfaces of constant  $\psi$  (i.e.,  $\frac{d}{ds} \equiv \hat{s} \cdot \nabla$ ).

Assume that  $\vec{E}$  has an asymptotic expansion of the form

$$\vec{E} = \sum_{n=0}^{\infty} \frac{1}{(ik)^n} \vec{E}_n. \quad \text{When this expansion is substituted into (A.4-1)}$$

and (A.4-2) the result is

$$\frac{d\vec{E}_n}{ds} + \frac{1}{2} \vec{E}_n \operatorname{div} \hat{s} = -\frac{1}{2} \nabla^2 \vec{E}_{n-1}, \quad (\text{A.4-3})$$

$$\hat{s} \cdot \vec{E}_n = -\text{div} \vec{E}_{n-1} \quad (\text{A.4-4})$$

where  $\vec{E}_{-1} = 0$ .

The coefficients  $\vec{E}_n$  are obtained recursively from these equations. One component of  $\vec{E}_n$  is given immediately by (A.4-4) while the other two components of  $\vec{E}_n$  are obtained by integrating (A.4-3). The integration is carried out along the rays (i.e., the orthogonal trajectories to the surfaces of constant  $\psi$ ). For large negative  $\psi$ ,  $\vec{E}_0$  is chosen to represent the incident plane wave, and all the other  $\vec{E}_n$  are chosen to be zero. The value of  $\vec{E}_n$  is then determined along any ray until that ray strikes the scattering surface. At the scattering surface the initial value of  $\vec{E}_n$  along the reflected ray is determined by  $\hat{n} \times \vec{E} = 0$  and  $\hat{s} \cdot \vec{E}_n = -\text{div} \vec{E}_{n-1}$  where  $\vec{E}$  is the sum of the fields on the incident and reflected rays and  $\hat{n}$  is the normal to the surface. When  $\vec{E}_0$  is determined as above, it gives just the geometric-optics approximation to the field.

Accuracy is guaranteed by this method only when the wavelength is small compared to the radii of curvature of the body. Furthermore the application of the Luneberg-Kline method used here applies only to bodies without any shadow region (i.e., the bodies must be infinite in extent) since the initial value of  $\vec{E}_n$  on a ray in the shadow region cannot be determined in the simple way shown above.

As an example this method can be applied to a paraboloid of revolution with the incident field incident along the axis of the body. Using polar coordinates, the equation of the paraboloid takes on the form

$$r = \frac{R}{1 + \cos \theta} \quad (\text{A.4-5})$$

The equation of the wave front is

$$\begin{aligned} \psi &= -r \cos \theta && (\text{before striking body}) \\ &= r - R && (\text{after striking body}). \end{aligned} \quad (\text{A.4-6})$$

Thus

$$\hat{s} = \begin{cases} -\cos \theta \hat{r} + \sin \theta \hat{\theta} & \text{(before striking body)} \\ \hat{r} & \text{(after striking body),} \end{cases} \quad (\text{A.4-7})$$

$$\text{div } \hat{s} = \begin{cases} 0 & \text{(before striking body)} \\ 2/r & \text{(after striking body).} \end{cases} \quad (\text{A.4-8})$$

If the incident field is polarized in the x-direction and is of unit amplitude, then, along the rays incident on the body

$$\vec{E}_i = \left\{ \sin \theta \cos \phi \right\} \hat{r} + \left\{ \cos \theta \cos \phi \right\} \hat{\theta} - \left\{ \sin \phi \right\} \hat{\phi} . \quad (\text{A.4-9})$$

Let  $\vec{E}_r$  denote the field along the reflected rays,

then  $\frac{d}{ds} = \frac{\partial}{\partial r}$ , and (A.4-3) and (A.4-4) take on the form

$$\frac{\partial \vec{E}_{or}}{\partial r} + \frac{1}{r} \vec{E}_{or} = 0, \quad (\text{A.4-3}')$$

$$\hat{r} \cdot \vec{E}_{or} = 0. \quad (\text{A.4-4}')$$

Using the boundary condition  $\hat{n} \times \vec{E} = 0$ , it follows that on the surface of the paraboloid

$$\hat{\phi} \cdot \vec{E}_{or} = \sin \phi \quad (\text{A.4-10})$$

$$\hat{\theta} \cdot \vec{E}_{or} = \cos \phi .$$

The solution of (A.4-3') subject to (A.4-4') and (A.4-10) is

$$\vec{E}_{or} = \frac{R}{r(1 + \cos \theta)} \left\{ [\cos \phi] \hat{\theta} + [\sin \phi] \hat{\phi} \right\} . \quad (\text{A.4-11})$$

It can be verified that  $\text{div } \vec{E}_{or} \equiv \nabla^2 E_{or} \equiv 0$ . Thus  $\vec{E}_{1r} = \vec{E}_{2r} = \vec{E}_{3r} = \dots = 0$ .

Therefore the Luneberg-Kline asymptotic expansion of the electric field is

$$\begin{aligned} \vec{E}_i e^{-ikr \cos \theta} + \vec{E}_{or} e^{ik(r - R)} \\ = \left\{ \hat{r} \sin \theta \cos \phi + \hat{\theta} \cos \theta \cos \phi - \hat{\phi} \sin \phi \right\} e^{-ikr \cos \theta} \end{aligned} \quad (\text{A.4-12})$$

$$+ \frac{R}{r(1 + \cos \theta)} \left\{ \hat{\theta} \cos \phi + \hat{\phi} \sin \phi \right\} e^{ik(r - R)}$$

which, as noted above, is just the geometric-optics expression. This expression is not only an asymptotic expansion of the field, but it is also the exact solution to the problem of axial scattering from a perfectly conducting paraboloid of revolution since the expression satisfies all of the necessary conditions. That is, if the right hand member of (A.4-12) is denoted by  $\vec{V}$ , then

- (1) the tangential component of  $\vec{V}$  vanishes on the surface of the paraboloid,
- (2) the divergence of  $\vec{V}$  is zero,
- (3)  $\vec{V}$  satisfies the vector Helmholtz equation:

$$\text{grad div } \vec{V} - \text{curl curl } \vec{V} + k^2 \vec{V} = 0,$$

and (4) the radiation condition is satisfied by  $\vec{V}$ .



APPENDIX 5

CROSS-SECTION FORMULAS FOR OTHER SURFACES\*

The methods of physical-optics have been applied to the problem of determining monostatic and bistatic radar cross-sections for surfaces other than those discussed in the body of this paper. Table 2 contains a partial list of the monostatic formulas.

TABLE 2  
OTHER APPROXIMATE MONOSTATIC CROSS-SECTION FORMULAS

Surface	Orientation of Surface and Radar	Cross-Section	Code to Symbols
Torus	Direction of propagation is parallel to the axis of the torus	$\sigma = 8\pi^3 R_1^2 R_2 / \lambda$	$R_1$ = distance from axis to center of ring $R_2$ = radius of ring
Flat Plate	Direction of propagation is normal to the surface	$\sigma = 4\pi W^2 H^2 / \lambda^2$	$W$ = width of plate $H$ = height of plate
Large Disc	Angle between direction of propagation and normal to disc given by $\theta$	$\sigma = \frac{4\pi}{\lambda^2} \left[ \frac{2\pi a^2 \cos \theta J_1(x)}{x} \right]^2$	$a$ = radius of disc $x = \frac{4\pi a}{\lambda} \sin \theta$

\*The formulas appearing in this appendix are valid for  $\lambda$  small with respect to the dimensions of the surface.

The D.S.P. theorem can be applied to the problem of determining  $\sigma_{a=i_y}^{\wedge}(\beta)$  for a variety of surfaces other than those discussed in the body of the paper. Table 3 contains a partial list of these formulas which were obtained using the geometry shown in Figure 3.

TABLE 3  
OTHER APPROXIMATE BISTATIC CROSS-SECTION FORMULAS

Surface	Geometry	Equation of Surface	$\sigma_{a=i_y}^{\wedge}(\beta)$
Ellipsoid		$\frac{X^2}{A^2} + \frac{Y^2}{B^2} + \frac{Z^2}{C^2} = 1$	$\frac{\pi A^2 B^2}{C^2} \cdot \frac{4}{\left[ (1 + \cos \beta) + \frac{B^2}{C^2} (1 - \cos \beta) \right]^2}, \beta < \pi$
One Branch of Hyperboloid of Two Sheets		$Z = -C \left[ 1 + \frac{X^2}{A^2} + \frac{Y^2}{B^2} \right]^{1/2}$	$\frac{\pi A^2 B^2}{C^2} \cdot \frac{4}{\left[ (1 + \cos \beta) - \frac{B^2}{C^2} (1 - \cos \beta) \right]^2}, \beta < 2 \tan^{-1} \left( \frac{B}{C} \right)$
Paraboloid (axis of symmetry is Z - axis)		$\frac{X^2}{A^2} + \frac{Y^2}{B^2} = -\frac{Z}{C}$	$\frac{\pi A^2 B^2}{C^2 (1 + \cos \beta)^2}$
Paraboloid (axis of symmetry is Y - axis)		$\frac{X^2}{A^2} + \frac{Z^2}{C^2} = \frac{Y}{B}$	$\frac{\pi A^2 C^2}{B^2 (1 - \cos \beta)^2}, \beta > 0$

## REFERENCES

1. "Studies in Radar Cross-Sections X - The Radar Cross-Section of a Sphere", by H. Weil, Willow Run Research Center, University of Michigan, (to be published).
2. The Mathematical Theory of Huygen's Principle, by B. B. Baker and E. I. Copson, 2nd Edition, Oxford University Press, (1950).
3. Symposium on Microwave Optics, Volumes I and II, The Eaton Electronics Research Laboratory, McGill University, Montreal, Canada, (1953).
4. Ibid, Vol. I "Calculation of the Echo Area of Several Scatterers of Simple Geometry by the Variational Method", by R. G. Kouyoumjian.
5. UMM-92, "Studies in Radar Cross-Sections IV - Comparison Between Theory and Experiment of the Cross-Section of a Cone", by K. M. Siegel, H. A. Alperin, J. W. Crispin, H. E. Hunter, R. E. Kleinman, W. C. Orthwein, and C. E. Schensted, Willow Run Research Center, University of Michigan, (February 1953).
6. The Theory of Sound, by J. W. S. Rayleigh, 2nd Edition, Dover Publications, New York, (1945).
7. "Kapazität von Strahlungsfeldern", by H. Weyl, Mathematische Zeitschrift, Volume 55, pp. 187-198, (1952).
8. "Zur Methode der Strahlungskapazität von H. Weyl", by C. Müller, Mathematische Zeitschrift, Volume 56, pp. 80-83, (1952).

## REFERENCES (Continued)

9. "On the Theory of Electromagnetic Wave Diffraction by an Aperture in an Infinite Plane Conducting Screen", by H. Levine and J. Schwinger, Communications on Pure and Applied Mathematics, Volume III, No. 4, p. 355, (December 1950).
10. CRL-R-E5070, "Back Scattering From Conducting Surfaces," by R. C. Spencer, Cambridge Research Laboratories, (April 1951).
11. TM-292, "Calculations of Echoing Area", by S. Milazzo, Federal Telecommunications Laboratory, (October 1947).
12. Electromagnetic Theory, by J. A. Stratton, McGraw Hill Book Co., New York, (1941).
13. UMM-87, "Studies in Radar Cross-Sections III - Scattering by a Cone", by K. M. Siegel and H. A. Alperin, Willow Run Research Center, University of Michigan, (January 1952).
14. Electromagnetic Waves, by S. A. Schelkunoff, D. Van Nostrand Co., New York, (1943).
15. Formulas and Theorems for the Special Functions of Mathematical Physics, by W. Magnus and F. Oberhettinger, Chelsea Publishing Co., (1949).
16. The Theory of Spherical and Ellipsoidal Harmonics, by E. W. Hobson, Cambridge University Press, (1931).
17. "Theoretical Study of Electromagnetic Waves Scattered From Shaped Metal Surfaces - Quarterly Report #3", by W. W. Hansen and L. I. Schiff, Microwave Laboratory, Department of Physics, Stanford University, (May 1948).
18. "An Asymptotic Solution of Maxwell's Equations", by M. Kline, Communications on Pure and Applied Mathematics, Vol. 4, p. 225, (1951).

REFERENCES (Continued)

19. Fourier Integrals, by G. A. Campbell and R. M. Foster,  
D. Van Nostrand Company, New York, (1951).
20. Mathematical Physics, by H. Jeffreys and B. S. Jeffreys,  
Cambridge University Press, (1950).

Distribution

Distributed in accordance with the Guided  
Missile Technical Information Distribution  
List; MML 200/3 No. 3, Parts A, B and C.